Mining Machines

(2023) VOLUME 41
ISSUE 3

QUARTERLY OF SCIENCE AND TECHNOLOGY

e-ISSN 2719-3306

Mining Machines

(2023) Vol. 41 Issue 3

KOMAG Research Institute

Quarterly of Science and Technology

October 2023

Pages 158-167

Volodymyr ANTONCHIK, Valentyn HANKEVICH, Sergiy MINIEIEV, Oleksandr PASHCHENKO, Valentyn BUKETOV

Method and tool for drilling and explosion well expansion in hard rocks

Pages 168-174

Tibor KRENICKY, Jozef MASCENIK, Tomas CORANIC, Juraj RUZBARSKY

Operating characteristics of bearings with magnetic nanoparticles doped lubricant

Pages 175-185

Janusz SMOLIŁO, Marek PIESZCZEK, Mieczysław LUBRYKA, Jerzy GRYCMAN

Technical aspects of liquidation of the shafts „Głowacki" in Rybnik, „Jas VI" and „Jas II" in Jastrzębie Zdrój, Poland

Pages 186-199

Volodymyr FALSHTYNSKYI, Andrii PERERVA, Vladyslav CHALYI, Vladyslav PSIUK, Roman DYCHKOVSKYI

Technical and technological support of the technology of activating the process of gasification of thin coal seams

Pages 200-211

Dmytro BABETS, Olena SDVYZHKOVA, Artur DYCZKO, Łukasz GLIWIŃSKI

Optimization of support parameters for reusable mining excavations based on a neuro-heuristic prognostic model

Pages 212-219

Mariusz WNĘK

Pressure analysis and control in an industrial gas heating furnace as a way to reduce CO_2 emission

KOMAG Institute of Mining Technology
Pszczyńska 37, 44-101 Gliwice, POLAND

miningmachines@komag.eu

OPEN ACCESS

CC BY NC

e-ISSN 2719-3306

https://doi.org/10.32056/KOMAG2023.3.1

Method and tool for drilling and explosion well expansion in hard rocks

Received: 14.06.2023

Accepted: 27.09.2023

Published online: 31.10.2023

Author's affiliations and addresses:

[1] Institute of Geotechnical Mechanics of National Academy of Sciences of Ukraine, 2a Simferopilska str., 49000, Dnipro, Ukraine

[2] Dnipro University of Technology, 19 Yavornytskoho Ave., 49005, Dnipro, Ukraine

[3] Universidad Nacional de San Agustin de Arequipa, San Agustin Street 107, 04000 Arequipa, Peru

*** Correspondence:**

e-mail: sergmineev@gmail.com

Volodymyr ANTONCHIK [1], Valentyn HANKEVICH [2], Sergiy MINIEIEV [2*], Oleksandr PASHCHENKO [2], Valentyn BUKETOV [3]

Abstract:

The paper represents the problem of expanding wells in hard and especially hard rocks. The general direction of solving this problem, the previous methods of solving it and their shortcomings are shown. A new method of drilling and blasting expansion of wells in strong and especially hard rocks is presented, using the energy of a directed explosion of low power to create a three-dimensional network of cracks in the rock mass around the well. The drawings of the tool for drilling and blasting expansion of wells in strong and especially hard rocks at the level of a draft design are given, and the calculation of the explosion energy of a single charge of explosives is carried out, and their mass necessary for such an explosion is determined.

Keywords: expand of wells, hard rocks, drilling, blasting, energy, directed explosion, rock mass, explosives

Publisher: **KOMAG Institute of Mining Technology, Poland**
© 2023 Author(s). This is an open access article licensed under the Creative Commons BY-NC 4.0 (https://creativecommons.org/licenses/by-nc/4.0/)

1. Introduction

It is known that the drilling of large diameter wells in strong and especially hard rocks is one of the main operations in the extraction of minerals. Despite a lot of research and development of drilling methods and tools, it still remains one of the most difficult, time-consuming and expensive parts of mining. Difficulties in drilling wells are especially noticeable when drilling large diameter wells in hard and very hard rocks, so the following solution to this problem was found. Initially, a small diameter well is drilled, which requires much less time and material costs. After that, this well is expanded to a larger diameter. In total, this takes much less time and money than direct drilling of a large diameter well. This is explained by the fact that when expanding an already drilled well, the destruction of the rock occurs as a result of tangential stresses on the free surface of the drilled well. This requires 5-10 times less energy consumption of the drilling tool than destroying the rock by pressing the tool into a monolithic mass, creating depressions in it in the form of holes (regrinding the rock to the state of sand and dust under the tool), destroying the rock because of normal compressive stresses and thus produce by drilling a well.

2. Methodology

Let's consider some of the main ways of expanding wells and their disadvantages.

There is a known method of expanding wells in rock with a mechanical tool (cutter or drill), which consists in drilling the rock by chipping it on the free surface of a pre-drilled well [1].

Since the zone of rock chipping goes from a larger diameter, where the rock is destroyed by cutters or chisels, to a smaller diameter of the leading cut, there is a need to compress the rock for its chipping on the surface of the pre-drilled well. This requires a little more effort and leads to the need to grind the entire volume of rock of the future well into small particles, which requires quite a lot of energy, time and replacement of expensive drilling tools and quite significant costs for the expansion of the well.

There is a well-known method of expanding wells using thermal devices [2], which consists in the fact that the entire volume of the rock of the future well is drilled thermally, that is, the upper layer of the rock is heated very quickly, which leads to its rapid expansion and separation from the unheated rock from effects of thermal stresses, after which particles of the separated rock are carried away by flows of the heat carrier (gas).

The disadvantage of this method is the significant expenditure of thermal energy from the combustion of fuel, which is used for the destruction and removal of rock by only 5÷10% (percentages), in addition, not all types of rock can be drilled by the thermal method due to the fact that with significant heating some of them start to melt, rock chipping stops and it is very difficult to remove their melt from the well.

There is a well-known method of thermomechanical expansion of wells [3], which consists in the fact that the rock is pre-heated to create stresses in it and then drilled with a mechanical tool, which reduces the effort to destroy the rock and the wear of the mechanical tool [4].

The disadvantage of this method is the significant cost of thermal energy for preliminary heating of the rock, which is used for heating, stress creation and destruction of various types of rocks by only 10-20% (percentages), which in total exceeds the energy costs and the total cost of expanding wells in comparison with mechanical method of expanding wells.

There is a known method of thermocyclic destruction of rocks, which consists in preliminary cooling of rocks [5] adjacent to the drilled well and formation of cracks in them as a result of compression of these rocks and lowering of their temperature, after which drilling of such fractured rock requires significantly less time and material costs. However, the implementation of this method of expanding wells requires rapid cooling of rocks to significant negative temperatures, which can only be done with the help of low-boiling liquids, for example, liquid nitrogen. Currently, the production of liquid nitrogen requires significant energy and material costs, which significantly increases the total cost of expanding the well.

Publisher: **KOMAG Institute of Mining Technology, Poland**
© 2023 Author(s). This is an open access article licensed under the Creative Commons BY-NC 4.0 (https://creativecommons.org/licenses/by-nc/4.0/)

The general disadvantages of thermomechanical expansion methods are a small volume of heated or cooled rocks due to their low thermal conductivity, which leads to significant costs of thermal energy or low-boiling coolant and low overall efficiency. drilling works when expanding wells.

Expansion of wells is also carried out by blasting [6], when several holes are drilled around the drilled well, which are charged with explosives and detonated. The destruction of the rock is mostly in the direction of the drilled well, which creates an expanded well with extremely uneven edges, which in the future is mainly used for the subsequent charging of explosives and explosions for the collapse of the rock mass during mineral extraction. This method [7,8] expansion of wells has a number of significant disadvantages. Thus, the drilling of several holes around the circumference of the well with a conventional mechanical tool requires significant material costs and time, as well as their subsequent charging and extraction of the destroyed rock from the expanded well. A particular difficulty is the extraction of destroyed rock from horizontal or dead-end vertical wells directed downwards. Therefore, this method of expanding wells is mainly used for expansion of emerging wells during mineral extraction.

It should be noted that one of the main disadvantages of the existing rock destruction by explosion is the mismatch of the direction of movement of the detonation and the accompanying shock wave with the direction of rock destruction. Thus, in the known methods of destruction of rocks by explosion [4] the detonation wave travels along the explosive charge in the direction of the central axis of symmetry along the well from the mouth to the surface of the bottom hole in the dead end of the well, while rock destruction occurs mainly in the radial direction to the axis of the well. This means that the primary destruction of the rock is not caused by the directed impact of the shock wave on the walls of the well, but by its reflected impact from the bottom hole or between explosive charges, as well as the effect of high pressure of gasified explosion products on the walls of the well. Such pressure acts in the radial direction, uniformly on all points of the surface of the well and, taking into account its correct cylindrical shape, creates a uniform (radius) field of normal compressive stress in the rock on the surface of the well, i.e. conditions of the most energy-intensive destruction of hard rocks. As a result, a significant part of the energy of the explosion is used to destroy the rock at the wall of the well to the level of sand and dust, and only after the field stress in the rock reaches the free surface at the mouth of the well, tangential stresses arise in the rock, which leads to significant destruction of the rock on the free the surface [9]. After the plug is removed and the well is depressurized, gasified explosion products under high pressure leave the well, which also reduces the efficiency. explosion, which in known methods of explosive destruction of rocks is no more than 20%. that leads to significant destruction of the rock on the free surface. After the plug is removed and the well is depressurized, gasified explosion products under high pressure leave the well, which also reduces the efficiency. explosion, which in known methods of explosive destruction of rocks is no more than 20%. that leads to significant destruction of the rock on the free surface. After the plug is removed and the well is depressurized, gasified explosion products under high pressure leave the well, which also reduces the efficiency. explosion, which in known methods of explosive destruction of rocks is no more than 20% [10].

3. Main material

As can be seen from the listed methods of expanding wells, the most common task is the initial loosening of rocks by creating a leading cavity (drilling a well of a small diameter) and the subsequent destruction of the rock in this leading cavity (mechanical method or further loosening of rocks around the drilled well using a drilled well (thermomechanical methods) However, the methods listed above for loosening the mass of rocks adjacent to the drilled leading well are sufficiently energy-intensive that in the conditions of the growing price of energy carriers, the cost of expanding wells in strong and especially strong rocks and the cost of mineral extraction significantly increases.

Due to the above-mentioned disadvantages of known methods of explosive destruction of rocks, ways to increase efficiency become obvious. explosive substance when destroying strong rocks.

1. The detonation and accompanying shock wave must be directed into the rock, i.e. in the radial direction and directly passes from the explosive to the rock without an air gap.

Publisher: **KOMAG Institute of Mining Technology, Poland**
© 2023 Author(s). This is an open access article licensed under the Creative Commons BY-NC 4.0 (https://creativecommons.org/licenses/by-nc/4.0/)

This will allow the energy of the detonation and the accompanying shock wave to be used for the preliminary destruction of rocks by creating cracks.

2. Explosive charges in the well must be separated and detonated independently of each other, successively from the wellhead to its dead end with a short delay in time.

   The directed explosion of the first discrete charge at the wellhead will create a stress field in the rock in the form of a torus, which, being near the free surface of the bottom hole, will create tangential stresses in the direction of the free surface of the bottom hole at the wellhead, which will lead to the destruction of the rock by creating a system of cracks in it. After that, the next explosive charge is detonated, which also creates a system of cracks on the free surface formed by the cracks of the first explosive charge. All subsequent explosive charges explode sequentially with the same time delay. This allows you to create a system of deep cracks in the rock without spending energy on its grinding.

3. The exit from the well should be closed as long as possible both after the first and subsequent explosive explosions. In this case, the gasified products of the explosion, which are under high pressure, will rush into the cracks in the rock created by the shock wave and will significantly increase both their depth and the cross-section of these cracks. In this case, the energy of the explosive explosion is used to the maximum.

   Based on this, the following method of drilling and blasting expansion of wells is proposed.

The problem of softening the rocks around the well can be solved quite effectively using an explosion in the radial direction (to the axis of the well) when the detonation wave in the charge of the explosive substance (ES) and the subsequent shock wave of the gasified products of the explosion pass directly into the rock of the well wall perpendicular to its surface and not in parallel, as it usually happens when an explosive charge explodes in a well.

Such directionality of the explosion makes it much more effective and requires much less explosives. An even greater efficiency of using this method of directional explosion can be achieved if the explosive charges are separated, placed sequentially in the well, and their successive short-delayed detonation from the mouth of the well to its bottom. Explosive charges in the well must be separated and detonated independently of each other, successively from the wellhead to its dead end with a short delay in time.

The directed explosion of the first discrete charge at the wellhead will create a stress field in the rock in the form of a torus, which, being near the free surface of the bottom hole, will create tangential stresses in the direction of the free surface of the bottom hole at the wellhead, which will lead to the destruction of the rock by creating a system of cracks in it. After that, the next explosive charge is detonated, which also creates a system of cracks on the free surface formed by the cracks of the first explosive charge. All subsequent explosive charges explode sequentially with the same time delay. This allows you to create a system of deep cracks in the rock without spending energy on its grinding, as it happens as a result of an explosion in known ways.

The exit from the well should be closed as long as possible after explosive explosions. In this case, the gasified products of the explosion, which are under high pressure, will rush into the cracks in the rock created by the shock wave and will significantly increase both their depth and the cross-section of these cracks. In the above-mentioned method, the energy of the explosion of explosives is used to the maximum and it goes only to the preliminary destruction of rocks by creating cracks in them, which requires significantly less explosives and allows creating a new method of drilling and blasting expansion of wells and a new drilling and blasting tool (Fig. 1÷5).

The following symbols are used in Fig. 1÷6:
1 – rocks; 2 – well; 3 – metal sleeve; 4 – rod; 5 – guide sleeve; 6 – disk spring; 7 – nut; 8 – emphasis; 9 – explosive charge; 10 – detonation cord; 11 – elastic sheath; 12 – electric wire; 13 – clay and crushed stone plug; 14 – two-way drilling auger; 15 – auger body; 16 – cutters of the auger body; 17 – conveyor screw.

Publisher: **KOMAG Institute of Mining Technology, Poland**
© 2023 Author(s). This is an open access article licensed under the Creative Commons BY-NC 4.0 (https://creativecommons.org/licenses/by-nc/4.0/)

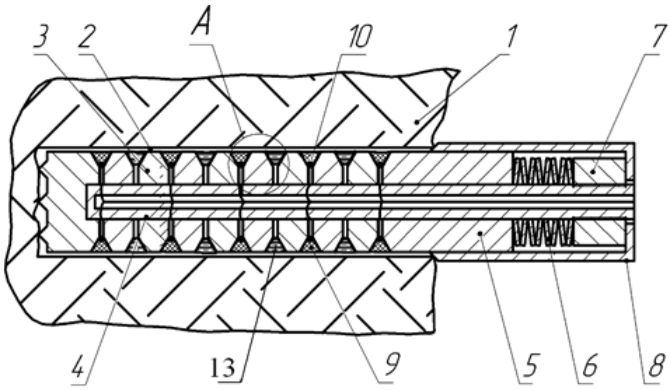

Fig. 1. Longitudinal section of a part of the device for drilling and blasting expansion of wells in the initial position

In Fig. 1 shows a longitudinal section of a part of the device for drilling and blasting expansion of wells in the initial position, the well being expanded and rocks.

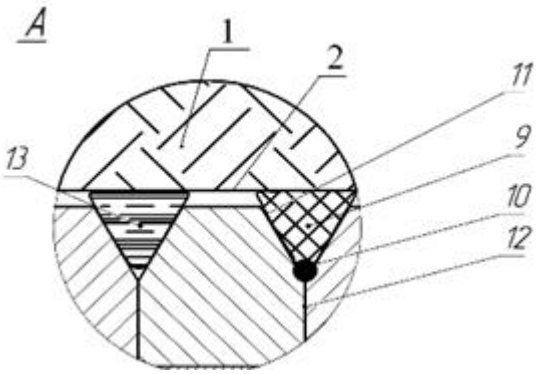

Fig. 2. Longitudinal section of an enlarged fragment of the explosive well expansion device in the initial position in the well

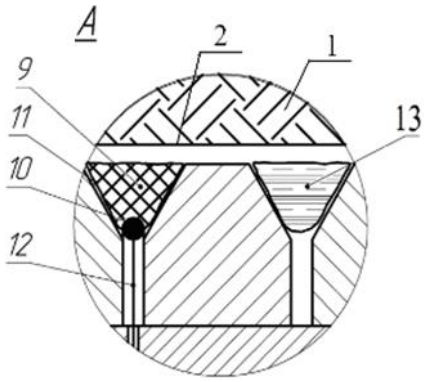

Fig. 3. Longitudinal section of an enlarged fragment of a blasting device for expanding wells in the working position

In Fig. 2 shows a longitudinal section of an enlarged fragment of the explosive well expansion device in the initial position in the well.

In Fig. 3 shows a longitudinal section of an enlarged fragment of a blasting device for expanding wells in the working position.

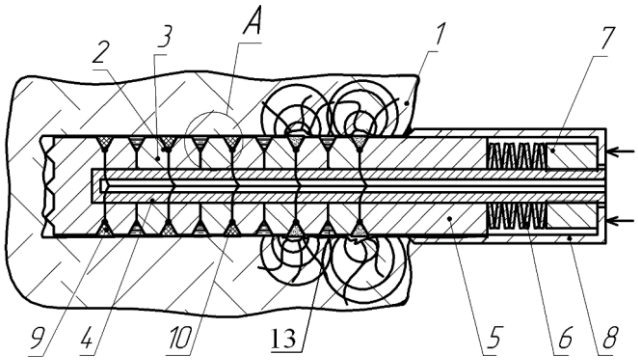

Fig. 4. Longitudinal section of the drilling and blasting device for expanding wells in the working position immediately after the detonation

Publisher: **KOMAG Institute of Mining Technology, Poland**
© 2023 Author(s). This is an open access article licensed under the Creative Commons BY-NC 4.0 (https://creativecommons.org/licenses/by-nc/4.0/)

In Fig. 4 shows a longitudinal section of the drilling and blasting device for expanding wells in the working position immediately after the detonation of two explosive charges and the expanded well in rock.

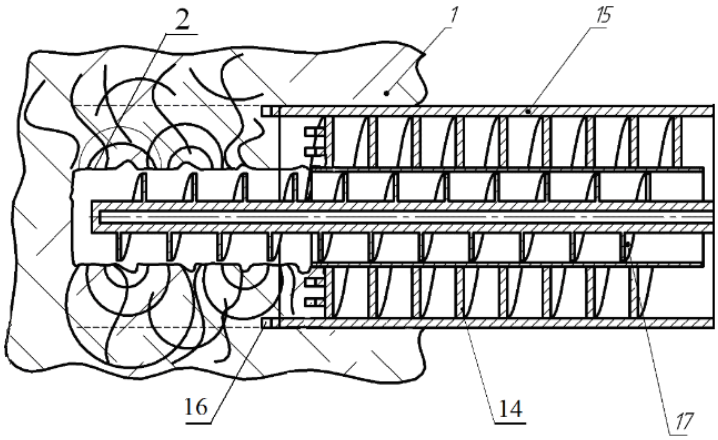

Fig. 5. Longitudinal section of the device for expanding the well after explosive explosions with a mechanical drilling tool

In Fig. 5 shows a longitudinal section of the device for expanding the well after explosive explosions with a mechanical drilling tool, for example, a two-way auger with cutters.

The method of blast expansion of wells is as follows. In a pre-drilled well, individual explosive charges 9 of small power are placed in a hermetic elastic shell 11 in the form of a toroidal cone with an electrodetonator and a detonating cord 10 at the top of the cone, separated from each other by metal bushings (Fig. 3). 1. Clay-crushed plugs 13 in a hermetic elastic shell 11 in the form of a toroidal cone are also located between the explosive charges, which are also located between the metal bushings 3, Fig. 2, 3. Next, the metal bushings 3 move along the axis of the well until they come into contact with each other, displacing part of the charges explosive substance 9 and clay-crushed plugs 13 to the contact with the walls of the well Fig. 2, 3. The well at the mouth is closed from the outside with a stopper 8, which, together with the metal bushings 3 and the guide bushing 5, is pressed with great force to the bottom with the help of hydraulic cylinders, and after that they perform a short-delayed detonation of explosive charges 9 with electric impulses that are fed through the electric wire 12 Fig. 4. The detonation of explosive charges 9 is carried out from the top of the cone of the toroidal shape of the charges, which allows you to direct the detonation and shock wave directly to the wall of the well into the rock without affecting the metal bushings between the charges. After detonation of the explosive charges 9, metal bushings 3 under the action of the pressure of the gases of the explosion products move in the direction of the mouth of the well, compressing the disk spring 6 that protects the instrument from destruction. After a drop in the pressure of the gases produced by the explosion, the metal bushings 3 are returned to their initial position by a plate spring 6, and a network of cracks appears in the rock around the well. Next, the external stop 8 is removed and the rod 4 with metal bushings 3 is removed from the well, and the volume of fractured rock is drilled and extracted from the expanding well with a mechanical drilling tool Fig. 5.

The device for explosive expansion of wells in rock works as follows. A well of a given diameter and length is mechanically drilled in rocks. A rod 4 is inserted into it, on which metal bushings 3 and a guide bushing 5 with equal gaps between them are installed, which are filled with explosive charges 9 in an elastic shell 11 with a detonation cord 10 and an electric detonator in it. Electrodetonators are pre-connected with an electric wire 12 for supplying electric current. Clay and crushed stone plugs 13 are placed between explosive charges 9 in conical toroidal elastic shells 11, between metal bushings 3. Disc springs 6, nut 7, Fig. 1, 2. After that, the nut 7 compresses the plate springs 6 and moves the guide sleeve 5 and the metal plugs 3 in the direction of the wellbore until all the metal sleeves 3 and the guide sleeve 5 are compressed against each other. After that, the stop 8 is installed on the guide sleeve 5 (Fig. 1, 4).

Publisher: **KOMAG Institute of Mining Technology, Poland**
© 2023 Author(s). This is an open access article licensed under the Creative Commons BY-NC 4.0 (https://creativecommons.org/licenses/by-nc/4.0/)

As a result of this movement of the metal plugs 3, the explosive charges 9 in the elastic casings 11 are partially pushed into the gap between the metal plugs 3 and the wall of the well 2 and create direct contact of the charges 9 with the walls of the well in the form of cylindrical rings, and the clay-crushed plugs 13 are partially pushed into the gap between metal bushings 3 and the wall of the well 2 and create clay and crushed stone plugs 13 between explosive charges 9 Fig. 3, 4. After that, stop 8 closes the gap between the guide sleeve 5 and the wall of the well 2. The explosive charge 9 is detonated first, closest to the wellhead. Next, successively, with some delay in time, all other charges of explosives are detonated in 9 Fig. 4. During the explosion of explosive charges 9 between the metal bushings 3, gasified explosive products create high pressure, but due to the fact that the metal bushings 3 can move along the rod 4, they are not destroyed and deformed, but move to the exit from the well, compressing the disk springs 6, and after reducing the pressure of the gasified products of the explosion, the metal bushings 3 return to their initial position. The explosions of explosive charges 9 create a three-dimensional network of cracks in the rock around the well 2, after which the drilling tool in the form of a double-entry drilling auger 14 starts drilling the fractured volume of the rock around the well 2 Fig. 5. Drilling begins with the immersion of 1 cutters of the auger body 16 into the rock, rotating with the body of the auger 15, which create a leading cut and separate part of the fractured rock volume around the well. Further, the cutters located on the spirals of the two-way drilling auger 14 destroy the fractured rock and it is transported by the two-way drilling auger 14 and the transport auger 17 outside the extended well.

After leveling the walls of the well, its expansion may continue with a similar device of a larger diameter. A set of blasting expanders of different diameters allows you to expand the well to the size of ventilation ducts or small workings in a horizontal, vertical or any other direction quite quickly and at low cost.

The main condition of the device's operation is the preservation of its structure after a series of explosions. Therefore, the total work of the impact of a single explosion on the details of the device should not lead to its destruction. That the work of the device parts must be in the area of elastic deformations and it can be calculated using Hooke's law. The most stressed part is the disk spring 6. The scheme of forces applied to the device and the deformation of a separate part are presented in Fig. 6.

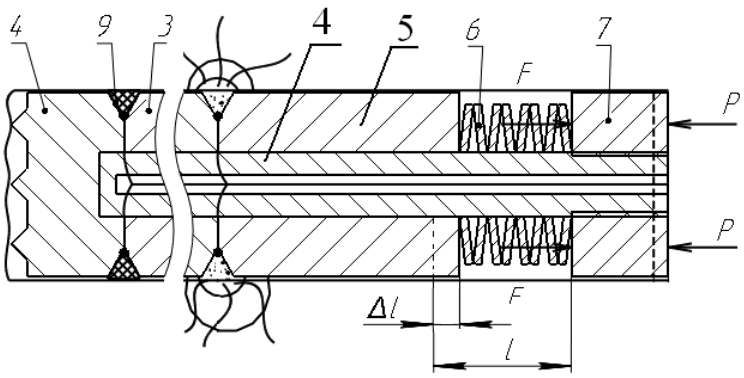

Fig. 6. Scheme of forces applied to the device and the deformation of a separate part

As is known from the course of physics, the elastic force arising from the linear deformation of an elastic element in this case of a spring is equal to:

$$F = k\Delta l \tag{1}$$

where:

F – the force compressing the spring, N,

k – coefficient of elasticity, N/m,

Δl – amount of spring deformation, m.

Publisher: **KOMAG Institute of Mining Technology, Poland**
© 2023 Author(s). This is an open access article licensed under the Creative Commons BY-NC 4.0 (https://creativecommons.org/licenses/by-nc/4.0/)

It is known that for each spring there is a limit deformation value Δlp, exceeding which will lead to the destruction of the spring. The elementary work of the elastic force is determined by the formula:

$$dA = F \cdot d(\Delta l) \tag{2}$$

Substituting (1) into (2), we get:

$$dA = k \cdot \Delta l \cdot d(\Delta l) \tag{3}$$

We determine the total work by the maximum allowable compression of the spring by integrating both parts of equation (3) $\int_0^A dA = \int_0^{l_n} k \cdot \Delta l \cdot d(\Delta l)$. we will get:

$$A_s = \frac{1}{2} \cdot k \cdot \Delta l_n^2 \tag{4}$$

where:

A_s – total work on the maximum allowable compression of the spring,

Δl_n – the maximum permissible deformation of the spring.

Thus, the work of the explosion of a unit charge should not exceed the total work of the maximum allowable compression of the spring.

$A_{\text{des}} \leq A_s$

Work on the destruction of the device is carried out as a result of the expansion of gaseous products of the explosion. However, not all the energy of the explosion passes into the pressure of the gasified products of the explosion. Part of the energy of the explosion goes into the rock together with the shock wave caused by the detonation of explosives and the movement of the products of the explosion in the direction of the detonation wave, so the total ideal work of the explosion A_{charge} should be 1.4÷1.6 times more work of expansion of gaseous products of the explosion, i.e. and A_{des}.

$$A_{charge} = A_{\text{des}}.\times (1.4 \div 1.6) \tag{5}$$

The ideal work of the $A_{id.es.ud}$ explosion is given in the reference literature in kilojoules per kilogram of explosive substance [6]. Divided A charge into $A_{id.es.ud}$ for the selected explosive, we get the mass of a unit explosive charge in the form of a truncated torus, which can be detonated without destroying the device.

$$m_{vc.charge} = \frac{\mathrm{A}_{charge}}{\mathrm{A}_{\mathrm{ud.ES}}} = \frac{[J]}{[J]/[kg]} = [kg] \tag{6}$$

Next, based on the density of the selected explosive, we determine the volume and dimensions of the toroidal cone of the charge.

The distance between the charges should be as minimal as possible, taking into account the clay plug.

The proposed method and device for drilling and blasting expansion of wells make it possible to significantly increase the speed of expansion of wells hard or especially hard rocks, as well as reduce the cost of drilling works account of the following factors.

The use of a directional explosion and its detonation and shock wave, which directly passes into the rock in the radial direction.

The use of separate charges of explosives to create a toroidal spherical field is tense near the free surface that is formed, which leads to successive stepwise destruction of the rock by the action of tangential tension on the free surface of the rock exposed by each explosion in the cracks that appear.

Publisher: **KOMAG Institute of Mining Technology, Poland**
© 2023 Author(s). This is an open access article licensed under the Creative Commons BY-NC 4.0 (https://creativecommons.org/licenses/by-nc/4.0/)

The use of a time delay in the detonation of charges for the formation of cracks and the operation of each subsequent charge on the "free" surface.

Limitation of charges with plugs and sealing of the well with an external plug for the formation of a directional explosion and greater work during the expansion of gasified products of the explosion, which are under high pressure, the efficiency of use of which in this case reaches up to 80%.

Drilling of rock destroyed by an explosion, which is reduced in its main mass (inside the leading cut) to loosening of fractured rock, which is tens of times cheaper than drilling of the same volume of solid monolithic rocks.

4. Conclusions

It should be noted that the main difficulty when drilling or expanding wells in strong or particularly strong rocks with a mechanical tool is the destruction of monolithic volumes of these rocks by the action of normal compressive stresses created by the tool, the values of which are the greatest for the destruction of strong or particularly strong rocks. In the case when there is a free surface in the zone of action of a mechanical tool (cutter or drill bit), (in front or from the side) the destruction of strong or particularly strong rocks occurs under the action of tangential stress (and in the case of fractured rock, they act in a thin layer) which for the destruction of strong rocks, it is many times less than the normal compressive stresses in the monolithic volume of the rock. In this method of drilling and explosive expansion of wells, well expansion drilling is performed on fractured rocks destroyed by an explosion, which is 5÷10 times faster and more economical (in terms of tool wear and energy consumption) compared to known methods of expanding wells with a mechanical tool.

Offered the method and device of drilling and blasting expansion of wells is much more effective and cheaper than all known methods of expanding wells in hard and especially hard rocks. Its efficiency increases even more in the case of repeated expansion of the well using this method and device, when the massif of rocks is already a network of holes that will be significantly increased by repeated exposure to a directed explosion, therefore offered the method and device for drilling and blasting expansion of wells is expedient to use repeatedly for expanding wells to the size of ventilation channels and small diameter workings.

References

[1] A.S. USSR No. 1452917 E21B 9/08, publ. 01/19/71, Bull. No. 27, Cone reaming bit, author: Yushko S. P.

[2] Brichkin A.V., Genbach A.N., Perevertun V.V., Roslyakova T.V.: New physical methods for the destruction of mineral environments, Nedra 1970, proceedings of the All-Union Conference Alma-Ata 1966. Fundamentals of the mechanism of thermal destruction of rocks

[3] A.S. USSR No. 188407 E 21 B 7/14 publ. 01.11.66 BI No. 22 Method of thermodynamic destruction of rock formations. V.E. Goryaev

[4] Sobolev, V., Bilan, N., Dychkovskyi, R., Caseres Cabana, E., & Smolinski, A. (2020). Reasons for breaking of chemical bonds of gas molecules during movement of explosion products in cracks formed in rock mass. International Journal of Mining Science and Technology, 30(2), 265–269. https://doi.org/10.1016/j.ijmst.2020.01.002

[5] Patent UA No. 86138 E21D 9/00 publ. 03/25/2009, bul. № 6 Method of molding a sverdlovinny charge of shaped charge for vibrating grinding of hot rocks, authors: Bulat A.F., Ishchenko K.S., Jos V.P., Osinniy V.Ya.

[6] Patent UA No. 39281 A E21B10/26 publ. 06/15/2001 Attachment for expansion of Sverdlovin Gavrich E.F., Inkin O.V.

[7] A. S. USSR No. 473814 E 21 C 21/10 publ. 09/18/75 BI No. 22 Device for thermomechanical drilling of wells. A.A. Galyas, N.M. Tregubov, N.M. Storozhuk

Publisher: **KOMAG Institute of Mining Technology, Poland**
© 2023 Author(s). This is an open access article licensed under the Creative Commons BY-NC 4.0 (https://creativecommons.org/licenses/by-nc/4.0/)

[8] Kozhevnykov A., Khomenko V., Liu B. C., Kamyshatskyi O., Pashchenko O.: The history of gas hydrates studies: From laboratory curiosity to a new fuel alternative. In Key Engineering Materials, Vol. 844, pp. 49-64. Trans Tech Publications Ltd. 2020

[9] Nikolsky V., Dychkovskyi R., Cabana E. C., Howaniec N., Jura B., Widera K., Smoliński A.: The Hydrodynamics of Translational−Rotational Motion of Incompressible Gas Flow within the Working Space of a Vortex Heat Generator. Energies, 15(4), 1431, 2022. https://doi.org/10.3390/en15041431

[10] Hankevich V. F., Pashchenko O. A., Kyba V. Ya.: Impact of vibrations on the drilling tool. Vibrations in engineering and technology, (4), 132-135, 2015

Publisher: **KOMAG Institute of Mining Technology, Poland**
© 2023 Author(s). This is an open access article licensed under the Creative Commons BY-NC 4.0 (https://creativecommons.org/licenses/by-nc/4.0/)

https://doi.org/10.32056/KOMAG2023.3.2

Operating characteristics of bearings with magnetic nanoparticles doped lubricant

Received: 19.07.2023

Accepted: 15.10.2023

Published online: 31.10.2023

Author's affiliations and addresses:

[1] Technical University of Kosice, Faculty of Manufacturing Technologies, Sturova 31, 08001 Presov, Slovak Republic

*** Correspondence:**

e-mail: tibor.krenicky@tuke.sk

Tibor KRENICKY [1*], Jozef MASCENIK [1], Tomas CORANIC [1], Juraj RUZBARSKY [1]

Abstract:

The main aim of the presented research was to investigate the operational characteristics of a bearing when alternative lubricants were used for comparison with a standard lubricant, including that containing magnetic nanoparticles. The bearing was subjected to varying operating conditions, differing in terms of mechanical load status. The monitoring of the bearing operation parameters primarily focused on monitoring the velocity and acceleration of vibrations, as well as the operating temperature of the bearing. The bearing with lubricant doped by magnetic nanoparticles exhibited reduced vibration velocity and acceleration values both under no load conditions and when subjected to a mechanical load. The operating temperature slightly increased during testing in the case of the bearing with nanoparticles compared to the bearing using the original lubricant.

Keywords: lubricant, magnetic nanoparticles, bearing, vibration

Publisher: **KOMAG Institute of Mining Technology, Poland**
© 2023 Author(s). This is an open access article licensed under the Creative Commons BY-NC 4.0 (https://creativecommons.org/licenses/by-nc/4.0/)

1. Introduction

The doping of nanoparticles as additives in lubricants can enhance their performance in various applications, such as the automotive industry, aerospace industry, heavy machinery and mining sector, producing so-called magnetic lubricants, or fluids [1-3]. Nanoparticles have the potential to improve wear resistance, reduce friction, and enhance lubrication properties. The advantageous properties of magnetic lubricants find numerous applications, and it is likely that their utilization within electromechanical devices is also promising [4]. Magnetic fluids are used in hydrodynamic bearings where they provide enhanced capacity and vibration damping [5]. Additionally, they reduce fluid leakage serving as a sealing mechanism [6].

Sealing with magnetic fluids offers significant advantages over seals made of solid materials. In comparison to conventional seals, like rubber parts on a shaft, magnetic fluid seals do not involve any friction between solid components, thereby eliminating the generation of particles from worn seals [7]. Magnetic seals can be utilized in dynamic applications, where, for example, a rotating shaft is sealed. In static applications, they seal mutually immobile components or parts [8].

The production of magnetic solutions typically involves a physicochemical process based on prolonged mechanical grinding of ferromagnetic particles, most commonly magnetite or ferrite, in the presence of a suitable surfactant. Subsequently, coarser particles are separated via centrifugation, a method known as wet grinding. However, this technique suffers from the drawback of being time-consuming, taking approximately 1,000 hours. To address this limitation, a faster and simpler method based on co-precipitation of metal salts in an aqueous solution is utilized [9, 10]. The size of the magnetic particles significantly influences the properties of magnetic fluids, necessitating the use of different magnetic fluids with distinct particle sizes in various industrial applications. For instance, larger particles that act as pure dipoles are required for optical applications, while small superparamagnetic particles are needed for NMR imaging.

The stability of a magnetic fluid depends on maintaining consistent chemical and physical properties throughout its volume. Achieving stability relies on a dynamic balance of several factors influencing the uniform dispersion of magnetic particles throughout the lubricant. These factors include the impact of thermal movement, magnetic moment, and stabilizing components [11, 12].

Thermal movement of molecules counteracts their spontaneous aggregation. However, at room temperature, it is often insufficient to compensate for dipole interactions, leading to particle aggregation. To prevent particles from approaching a critical distance, stabilizing additives are introduced. As the position of magnetic particles in the liquid is not fixed but subject to Brownian motion, interactions of their magnetic moments become enhanced, resulting in particle attraction and spontaneous aggregation, which is an undesirable phenomenon for magnetic lubricant stability. The aggregation is limited by the closest distance at which particles can approach each other. The potential energy decreases as the distance decreases, reaching its minimum value when particles come into contact. A surfactant, being an amphiphilic molecule with polar and non-polar parts, plays here a vital role. In a non-polar environment, the presence of a surfactant enhances the solubility of magnetic particles and stabilizes them. The surfactant forms a monomolecular layer on the particle's surface, with its polar part oriented towards the particle and its non-polar part interacting with the non-polar solvent. In a polar environment, a second layer is required, with the non-polar part oriented towards the non-polar part of the first layer and the polar part interacting with the carrier liquid. This arrangement effectively increases the minimum distance at which two coated particles can approach each other, preventing particle aggregation [13]. The surfactant's monomolecular and bipolar bilayer acts as a spherical barrier in the interaction of the magnetic moments of the particles and hinders particle aggregation. The bipolar double layer carries a group of charges on its surface, contributing to the electrostatic repulsion of the coated particles.

Whereas the usage of ferrofluids in hydrodynamic bearings offers several advantages, including increased bearing capacity and vibration damping, reduced fluid leakage, and the bearing functioning as a seal [14, 15] the primary objective of the presented research is to investigate the operational

Publisher: **KOMAG Institute of Mining Technology, Poland**
© 2023 Author(s). This is an open access article licensed under the Creative Commons BY-NC 4.0 (https://creativecommons.org/licenses/by-nc/4.0/)

characteristics including vibration and temperature of the common type of bearing when employing a lubricant containing magnetic nanoparticles as an alternative to the standard lubricant.

2. Experimental materials and methods

The lubricant containing nano-additives was synthesized at the IEP SAS in Kosice, comprising three primary constituents. The first component is a commercially available lubricant, SKF LGWA 2/0.2. The second component consists of magnetite nanoparticles coated with a layer of oleic acid, which constitutes the third component of the magnetic lubricant.

The preparation of the magnetic lubricant involved a three-step process (Fig. 1). Within the initial step, magnetic nanoparticles were synthesized using the chemical co-precipitation method. A solution containing ferrous Fe^{2+} ($FeSO_4.7H_2O$) and ferrous Fe^{3+} ions ($FeCl_3.6H_2O$) in a molar ratio of 1:2 was heated to 80°C. Addition of ammonium hydroxide to this solution led to the precipitation of iron ions and the formation of magnetite nanoparticles.

The second step involved the coating of the precipitated nanoparticles with oleic acid surfactant at a temperature of 82°C. Chemisorption of oleic acid molecules occurred on the nanoparticle surfaces, creating a spatial barrier between the particles, with a thickness of approximately 4 nm. The coated nanoparticles underwent multiple washing steps with distilled water and acetone to eliminate unreacted salts and unbound oleic acid residues. During washing, magnetic decantation with the use of a magnet was employed to separate and retain the magnetic nanoparticles, while the non-magnetic residue was removed by pouring out.

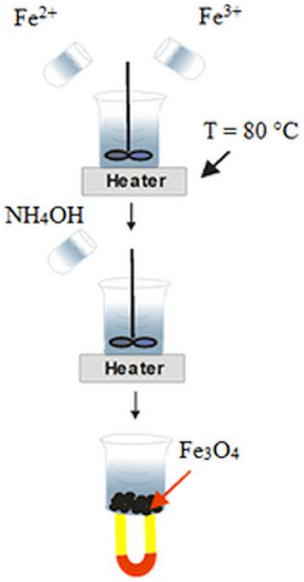

Fig. 1. Principle of magnetic nanoparticles synthesis by chemical co-precipitation

In the third preparation step, the pure SKF LGWA 2/0.2 lubricant was mixed with the coated nanoparticles. The two components were mixed in a 1:1 ratio at a temperature of 70°C until a homogeneous nanocomposite was achieved [2, 16].

To assess the performance of the lubricants, SKF 6205 ETN9 bearings were chosen [17]. Experiments were conducted at the laboratory stand (Fig. 2) of the Centre for Testing and Monitoring of Technical Systems at the Faculty of Manufacturing Technologies, Technical University of Kosice [18, 19]. The bearing was mounted using a steel intermediate piece to the output shaft of the SIEMENS 1LA7090-2AA10-Z electric motor with a power of 1.5 kW/50 Hz and a maximum rotational speed of 3000 rpm.

Publisher: **KOMAG Institute of Mining Technology, Poland**
© 2023 Author(s). This is an open access article licensed under the Creative Commons BY-NC 4.0 (https://creativecommons.org/licenses/by-nc/4.0/)

Fig. 2. Test bearings mounted on the experimental stand

Three types of bearings were subjected to testing. The first set of bearings consisted of those with the original lubricant applied during the manufacturing process. For the second set of bearings, a magnetic lubricant weighing 1.5 g was used. Prior to the application of the magnetic lubricant, the original bearings underwent a dismantling process to remove the bearing cage, followed by a degreasing bath to eliminate the original lubricant [20]. Subsequently, the magnetic lubricant was applied to the bearings, and after reassembling the bearing cage, the bearings were securely affixed to the test stand, ready for testing.

3. Experimental results

The bearing lubricated with the manufacturer's standard lubricant was assessed under the following conditions: without load and with a 30 kg load at a constant speed of 3000 rpm. When measured without the load, the CMMS Checker device recorded effective value of vibration velocity values of approximately 20 mm/s on both stands. The vibration acceleration in the unloaded bearings averaged around 6.8 g. Upon loading the bearings, the vibration velocity values decreased by an average of 64.5%. The vibration acceleration with a loaded bearing on the M1 engine decreased by 46.9%. However, for the M2 engine, the vibration acceleration increased by 0.6 g. The vibration velocity observed was likely due to the slightly unbalanced output shaft of the electric motor, which diminished after applying a 30 kg weight load on both stands.

A comparison of the bearings containing original and magnetic lubricant showed distinct behaviours of velocity and acceleration of vibrations as depicted in Table 1. The measured average vibration velocity for unloaded bearings was 47.5% lower for the bearing with magnetic lubricant than for the bearing with the original lubricant. As for vibration acceleration values, the bearing with magnetic lubricant exhibited lower values by 81.25% compared to the bearing with the original lubricant.

Table 1. Comparison of the vibrations of the bearing with original lubricant, with SKF LGWA 2/0.2 lubricant and the LGWA 2/0.2 lubricant doped with magnetic nanoparticles

	Velocity [mm/s]	**Acceleration [g]**
Original lubricant from the manufacturer without load	20.4	6.4
Original lubricant from the manufacturer with load 30 kg	7.8	3.4
SKF LGWA 2/0.2 lubricant without load	17.4	7.5
SKF LGWA 2/0.2 lubricant with load 30 kg	6.9	1
Magnetic lubricant without load	9.5	1.2
Magnetic lubricant with load 30 kg	4	1.6

Publisher: **KOMAG Institute of Mining Technology, Poland**
© 2023 Author(s). This is an open access article licensed under the Creative Commons BY-NC 4.0 (https://creativecommons.org/licenses/by-nc/4.0/)

Regarding the operating temperature, on the bearing with magnetic lubricant an average temperature of 33.1°C was detected, which represented an increase of 6.7°C when compared to the bearing with the original lubricant. During the measurement, the average temperature of the bearing with the original lubricant was 26.4°C. This rise in temperature can be attributed to the presence of magnetite nanoparticles in the magnetic lubricant. It is plausible that the rotation of the bearing causes the magnetite nanoparticles in the lubricant to rub against each other, leading to a slight temperature increase [21].

The measurements conducted on bearings with a load of 30 kg demonstrated a more significant reduction in both vibration velocity and acceleration compared to unloaded bearings. Specifically, the measured values of velocity and acceleration of vibrations for the loaded bearing with magnetic lubricant were 51.3% lower than those for the bearing with the original lubricant. During testing, the operating temperature of the loaded bearings with magnetic lubricant averaged at 31.4°C, while the temperature of the loaded bearings with the original lubricant was on average 4°C lower, reaching 27.2°C.

The comparison between bearings with SKF LGWA 2/0.2 and magnetic lubricant, under both no-load and loaded conditions, revealed notable differences. In the case of unloaded bearings, the bearing with magnetic lubricant exhibited values up to 45.4% lower than the bearing with SKF LGWA 2/0.2 lubricant. The operating temperature of the bearing with magnetic lubricant during no-load testing reached an average value of 31.1°C, while the bearings with SKF LGWA 2/0.2 lubricant had an average operating temperature of 30.0°C without load.

After testing both bearings with a 30 kg load and evaluating the average values, the bearing with magnetic lubricant displayed measured vibration velocity values 37.5% lower than the bearing with LGWA lubricant. In this scenario, the bearing with SKF LGWA 2/0.2 lubricant exhibited acceleration values 37.5% lower than the bearing with magnetic lubricant. Following the loading, the operating temperature of the bearing with magnetic lubricant averaged at 32.1°C, whereas the bearing with SKF LGWA 2/0.2 lubricant maintained an average temperature of 30.5°C.

After an hour's operation of the bearings under load, the measured average values of the vibration speed were unchanged. The average values of the vibration acceleration of the bearing with magnetic lubricant were reduced by 0.5 g, which is a difference of 17.9%. The operating temperature of loaded bearings with magnetic lubricant was on average 37.2°C after one hour of operation. The temperature of the bearing with SKF LGWA 2/0.2 lubricant was 32.4°C after one hour of operation.

The measured average values after a 10-hour test operation do not differ much from each other. The bearing with SKF LGWA 2/0.2 lubricant gives vibration velocity values of 4.2 mm/s and the bearing with magnetic lubricant gives 4.6 mm/s, a difference of 8.7%. Regarding average vibration acceleration values, the bearing with magnetic lubricant has values 33.4% higher than the bearing with LGWA 2/0.2 lubricant. The operating temperature after 10 hours of operation reached an average temperature of 35.7°C for the bearing with magnetic lubricant. A lower temperature was measured on the bearing with SKF LGWA 2/0.2 lubricant at an average level of 29.8°C.

4. Conclusion

The objective of this study was to develop a lubricant containing magnetic particles from a readily available standard lubricant and apply it to a rolling ball bearing. The commercial lubricant SKF LGWA 2/0.2 and the ball bearing 6205 ETN9 were chosen for testing purposes. The magnetic lubricant was created by incorporating magnetite nanoparticles into the SKF LGWA 2/0.2 lubricant for research purposes.

The bearings were subjected to a load of 30 kg and tested with three different lubricants. The first test involved bearings with the standard lubricant provided by the manufacturer. The second test utilized SKF LGWA 2/0.2 lubricant, while in the third variant, the bearing was treated with the lubricant containing magnetite nanoparticles. The CMMS Checker diagnostic tool and an infrared digital thermometer were employed to obtain measurements of the loaded and unloaded bearings.

Publisher: **KOMAG Institute of Mining Technology, Poland**
© 2023 Author(s). This is an open access article licensed under the Creative Commons BY-NC 4.0 (https://creativecommons.org/licenses/by-nc/4.0/)

The tests were conducted after 10 minutes of operation, during which the improved properties of the bearing with the magnetic lubricant were evident. Further testing was performed after one hour and 10 hours of operation. The results indicated that after these intervals, only minimal differences were observed between the measured values.

In all scenarios, the bearing with the magnetic lubricant exhibited lower measured values of vibration velocity and acceleration, both before and after loading. The operating temperature during testing showed a slight increase for the bearing with the doped lubricant in comparison to bearings with the original lubricant. On average, the temperature rose by approximately 5°C. This increase in temperature can be attributed to the presence of magnetic nanoparticles in the lubricant, which undergo friction with each other during rotation. The reduction in velocity and acceleration of vibrations can be attributed to the magnetic lubricant's higher density, which effectively dampens vibrations.

Acknowledgments

This work was supported by the Slovak Ministry of Education within project VEGA No. 1/0823/21.

References

[1] Wang P., Hang J., Wei S.: Analysis of Torque in Magnetorheological Rotary Brake. Advanced Materials Research, vols. 239-242, pp. 2297-2301, 2011

[2] Wang X., Lu W., Li H., Meng G.: A magnetorheological fluid lubricated floating ring bearing and its application to rotor vibration control. J. Vib. Shock, vol. 36, pp. 18–24, 2017

[3] Rosensweig R. E.: Ferrohydrodynamics. Courier Dover Publications, 1997

[4] Nikitin Y.: Diagnostics of BLDC motor winding based on a model approach in the state space. IOP Conference Series: Materials Science and Engineering, 2020, 971(4), 042101. Modelling of technical systems. CAD / CAM / CAE – technologies. doi:10.1088/1757-899X/971/4/042101. ISSN 1757-899X

[5] Zapomel J., Ferfecki P.: A new concept of a hydrodynamic bearing lubricated by composite magnetic fluid for controlling the bearing load capacity. Mech. Syst. Signal Pract., vol. 168, 108678, 2022

[6] Potoczny M., Zachara B.: Influence of magnetorheological fluid volume onto obtained critical pressures on rotary shaft seals. Key Engineering Materials, vol. 490, pp. 119-127, 2012

[7] Xie X., Dai Q., Huang W., Wang X.: Supporting capacity of a ferrofluid ring bearing. J. Phys. D Appl. Phys., vol. 54, 175004, 2021

[8] Petrigac M.: Diagnostics of the operation of the technical system when applying lubricant with magnetic nanoparticles. Diploma Thesis. Prešov, FMT TUKE, 2018, 67 p.

[9] Vekas L., Bica D., Avdeev M.V.: Magnetic nanoparticles and concentrated magnetic nanofluids: Synthesis, properties and some applications. China Particuology, vol. 5, no. 1–2, pp. 43–49, 2007

[10] Charles S. W.: The Preparation of Magnetic Fluids, in Ferrofluids, S. Odenbach (Ed.). Berlin: Springer Berlin Heidelberg, 2003, pp. 3–18

[11] Vekas L., Avdeev M.V., Bica D.: Magnetic Nanofluids: Synthesis and Structure, in NanoScience in Biomedicine, D. Shi (Ed.). Berlin: Springer Berlin Heidelberg, 2009, pp. 650–728

[12] Patel J.R., Deheri G.: Viscosity variation effect on the magnetic fluid lubrication of a short bearing. J. Serb. Soc. Comput. Mech., vol. 13, pp. 56–66, 2019

[13] Bee A., Massart R., Neveu S.: Synthesis of very fine maghemite particles". Journal of Magnetism and Magnetic Materials, pp. 6–9, Aug. 1995

[14] Khalil A., Nabhani M, Khlifi M.E.: Rotational viscosity effect on the stability of finite journal bearings lubricated by ferrofluids". J. Braz. Soc. Mech. Sci., vol. 43, 548, 2021

[15] Bialy W., Ruzbarsky J.: Breakdown cause and effect analysis. Case study. Management systems in production engineering, vol. 26, pp. 83-87, 2018

Publisher: **KOMAG Institute of Mining Technology, Poland**
© 2023 Author(s). This is an open access article licensed under the Creative Commons BY-NC 4.0 (https://creativecommons.org/licenses/by-nc/4.0/)

[16] Salwinski J., Horak W.: Measurement of normal force in magnetorheological and ferrofluid. Key Engineering Materials, vol. 490, pp. 25-32, 2012

[17] SKF Group: Deep groove ball bearings. http://www.skf.com/group/products/bearings-units-housings/ball-bearings/deep-groove-ball-bearings/deep-groove-ball-bearings/index.html?designation=6205%20ETN9

[18] Krenicky T.: Implementation of Virtual Instrumentation for Machinery Monitoring. In: Scientific Papers: Operation and Diagnostics of Machines and Production Systems Operational States: Vol. 4, RAM-Verlag, Lüdenscheid, 2011, pp. 5-8. ISBN 978-3-942303-10-1

[19] Krenicky T.: The Monitoring of Technical Systems Operation Using Virtual Instrumentation. Strojarstvo extra, 2010, No. 5, pp. 25/1-25/2. ISSN 1335-2938. (In Slovak)

[20] Turygin Y., Bozek P., Abramov I., Nikitin Y.: Reliability Determination and Diagnostics of a Mechatronic System. Advances in Science and Technology. Vol. 12, No. 2, June 2018, pp. 274–290. DOI: 10.12913/22998624/92298. ISSN 2299-8624

[21] Peterka J., Bozek P., Nikitin Y.: Diagnostics of automated technological devices. MM Science Journal, October 2020, pp. 4027-4034. DOI: 10.17973/MMSJ.2020_10_2020051. ISSN 1803-1269, 1805-0476

Publisher: **KOMAG Institute of Mining Technology, Poland**
© 2023 Author(s). This is an open access article licensed under the Creative Commons BY-NC 4.0 (https://creativecommons.org/licenses/by-nc/4.0/)

https://doi.org/10.32056/KOMAG2023.3.3

Technical aspects of liquidation of the shafts "Głowacki" in Rybnik, "Jas VI" and "Jas II" in Jastrzębie Zdrój, Poland

Received: 06.05.2023

Accepted: 02.07.2023

Published online: 31.10.2023

Author's affiliations and addresses:

[1] SRK S.A. w Bytomiu
ul. Strzelców Bytomskich 207,
41-914 Bytom, Poland

[2] SRK S.A. Oddział KWK „Jas-Mos-Jastrzębie III" ul. Górnicza 1,
44-330 Jastrzębie Zdrój, Poland

[3] SITG Koło „Anna" w Pszowie,
Oddział Rybnik, Poland

*** Correspondence:**

e-mail: grycman1960@gmail.com

Janusz SMOLIŁO [1], Marek PISZCZEK [1], Mieczysława LUBRYKA [2], Jerzy GRYCMAN [3*]

Abstract:

Mining plants liquidating the unnecessary objects, especially shafts, encounter difficulties related mainly to the selection of appropriate technology. In this material, we present solutions for two more difficult cases. The first consists in liquidating the shaft without making dams and maintaining the water permeability of the backfilling (Głowacki shaft), while the second one is the liquidation of the shaft, leaving the ladder compartment, pipelines and with the so-called artificial bottom which is in the shaft (Jas II shaft).

Keywords: shaft liquidation, backfilling column, backfill material

Publisher: **KOMAG Institute of Mining Technology, Poland**
© 2023 Author(s). This is an open access article licensed under the Creative Commons BY-NC 4.0 (https://creativecommons.org/licenses/by-nc/4.0/)

1. Introduction

The SRK branch in Jastrzębie Zdrój was established on October 1, 2016 as KWK "Jas-Mos". Its task, in the first place, was to liquidate, among others, the "Jas II" and "Jas "VI" shafts and then the "Jas I" and "Jas IV" shafts. On December 2, 2016, the activity of the branch was expanded to include part of the area of KWK Rydułtowy I and since then the branch has been operating in a two-branch structure with the Ruch "Jas-Mos" and the Ruch "Rydułtowy 1" branches. Tasks realized in the Rydułtowy I included: liquidation of some redundant and unsuitable for development buildings and liquidation of the entire underground infrastructure, including the liquidation of two shafts, i.e. the "Leon III" shaft in Rydułtowy and the "Głowacki" shaft in Rybnik. The restructuring process of Ruch "Rydułtowy I" was finally completed on December 31, 2021. In the following year, on 1 January, the Jastrzębie III mine was added to the SRK Branch in Jastrzębie Zdrój, which since then formed the Ruch "Jastrzębie III" of the Branch "Jas-Mos-Jastrzębie III" KWK mine and this organizational and legal status has existed to this day (1.05 2023).

2. Methods

This article discusses technical issues related to liquidation of the "Głowacki" shaft in Ruch "Rydułtowy I" and the "Jas II" and partly "Jas VI" shafts.

2.1. Liquidation of the “Głowacki” shaft

The SRK branch in Jastrzębie Zdrój, together with the creation of the Ruch "Rydułtowy I", received for liquidation two shafts together with their underground and surface infrastructure – the "Leon III" shaft in Rydułtowy and the "Głowacki" shaft in Rybnik - Niewiadom. The "Leon III" shaft was liquidated at first, the liquidation technology was similar to the technological process [1, 2] of the "Jas VI" shaft discussed later in the article. The decision to proceed with the immediate liquidation of the "Głowacki" shaft was made after an analysis of the technical condition of the shaft steelworks. The "Głowacki" shaft originally was used as a ventilation shaft, and after the fan station was liquidated and reinforced, it served mainly as an intake shaft, which was a way for water to run off from each water reservoir. This water was further captured in underground workings by the main drainage system of PGG S.A. KWK "ROW" Ruch Rydułtowy mine. To ensure the safety of the present and future coal mining, an extremely important issue was to maintain stable water ratios, i.e. underground water runoff routes and their intakes. It was of great importance to design the liquidation of the shaft in such a way as not to disturb and maintain the current migration of water in the rock mass in the vicinity of the shaft [3, 4]. It should also be noted that the nearby "Kościuszko" shaft, which was liquidated earlier, was also supposed to be a water runoff route, but already at the stage of its liquidation, the filling was sealed and from that time all water was discharged only through the "Głowacki" shaft. The amount of water flowing into the workings of KWK "ROW" Ruch Rydułtowy mine was also variable and depended on weather conditions. Regardless of the underground conditions, there were limitations on the surface related to the fact that the shaft was located in the Historic Mine Ignacy, and the shaft building itself was included in the register of immovable monuments of the Silesian Voivodeship since 2005. The "Głowacki" The shaft has a shaft landing and a steel, single-bolt hoisting tower built in 1901, reinforced in 1947, with a rivet-welded structure made of cylindrical profiles. Details of the liquidation project and technological arrangements were discussed on an ongoing basis with representatives of the Consultative Team appointed by the President of the city of Rybnik. In 2019, Mines Restructuring Company SA (SRK) commenced implementation of the project with the acronym TEXMIN. The TEXMIN (The Impact of Climate Change on Closed and Abandoned Mines) project, co-financed by the Research Fund for Coal and Steel, was implemented by an international consortium of the following partners: the Silesian University of Technology and SRK from Poland, the University of Exeter from Great Britain, the CERT Research Center from Greece, the Brown Coal Research Institute from the Czech Republic, Subterra Ingenieria from Spain and DMT from Germany with the Central Mining Institute (GIG) as the project coordinator. As part of the TEXMIN project, a team of scientists from the Central Mining

Publisher: **KOMAG Institute of Mining Technology, Poland**
© 2023 Author(s). This is an open access article licensed under the Creative Commons BY-NC 4.0 (https://creativecommons.org/licenses/by-nc/4.0/)

Institute and the SRK S.A. Working Group. The Department of KWK "Jas-Mos-Rydułtowy I" Ruch Rydułtowy I, under the leadership of the Chief Mining Engineer, developed a project for liquidation of the "Głowacki" shaft, taking into account the change in weather conditions as well as defined the requirements for the backfill regarding its water permeability.

Main technical parameters and geological-and-engineering conditions:

- shaft depth 625 m,
- cross-section of the shaft was uneven, from barrel (0.0 m - 115 m) through rectangular (115 m - 200 m) to circular (200 m - 625 m), and the cross-section area ranged from 14.4 m^2 to 18.3 m^2,
- type of the shaft lining is not uniform along the length of the shaft pipe. The section from the ground to the depth of 400 m was made in a brick wall casing. The remaining section was made in a masonry casing made of bentonites. The shaft documentation does not contain any information on the strength parameters of the lining material and the brand of the mortar used to make it.

Table 1. Shaft inlets and insulation dams in “Głowacki” shaft [5]

Depth [m]	Inlet	Type of a dam
0.00	Shaft outset	--
10.50	Ventilation telescope I	Wall dam. Telescope liquidated
33.00	Ventilation telescope II	Wall dam. Telescope liquidated
150.00	Level 150	Wall insulation dam
200.00	Level 200	Wall insulation dam
240.00	Level 240	Wall insulation dam
300.00	Level 300	Wall insulation dam
350.00	Level 350	Wall insulation dam
393.00	Pipe telescope	Wall insulation dam
400.00	Level 400	Wall insulation dam
455.00	Level 455	Wall insulation dam
584.00	Inlet to the seam 620/1-2	Wall insulation dam
594.34	Level 600	Wall insulation dam

The liquidated inlets to each level in the "Głowacki" shaft were closed with insulating wall dams. Due to the lack of access to the above-mentioned dams at each shaft level, it was impossible to determine their dimensions, thickness and technical condition of the wall based on the on-site inspection. In this situation, the location of the dams listed in Table 1 above and their dimensions were adopted on the basis of the available archival documentation.

Hydro-geological conditions

Amount of water inflow to the "Głowacki" shaft in 2009÷2016 ranged from **0.95÷-1.67 m^3/min**. Since 2018, the water inflow to the shaft has stabilized at the level of approximately 1.10 m^3/min, and the rate of water flowing directly into the shaft from the levels of 150 m, 200 m, 240 m, 300 m and 400 m and leaking from the shaft lining flows down the shaft cross-section (at the level of 600 m, is observed as a torrential rain in the entire cross-section of the shaft.

Publisher: **KOMAG Institute of Mining Technology, Poland**
© 2023 Author(s). This is an open access article licensed under the Creative Commons BY-NC 4.0 (https://creativecommons.org/licenses/by-nc/4.0/)

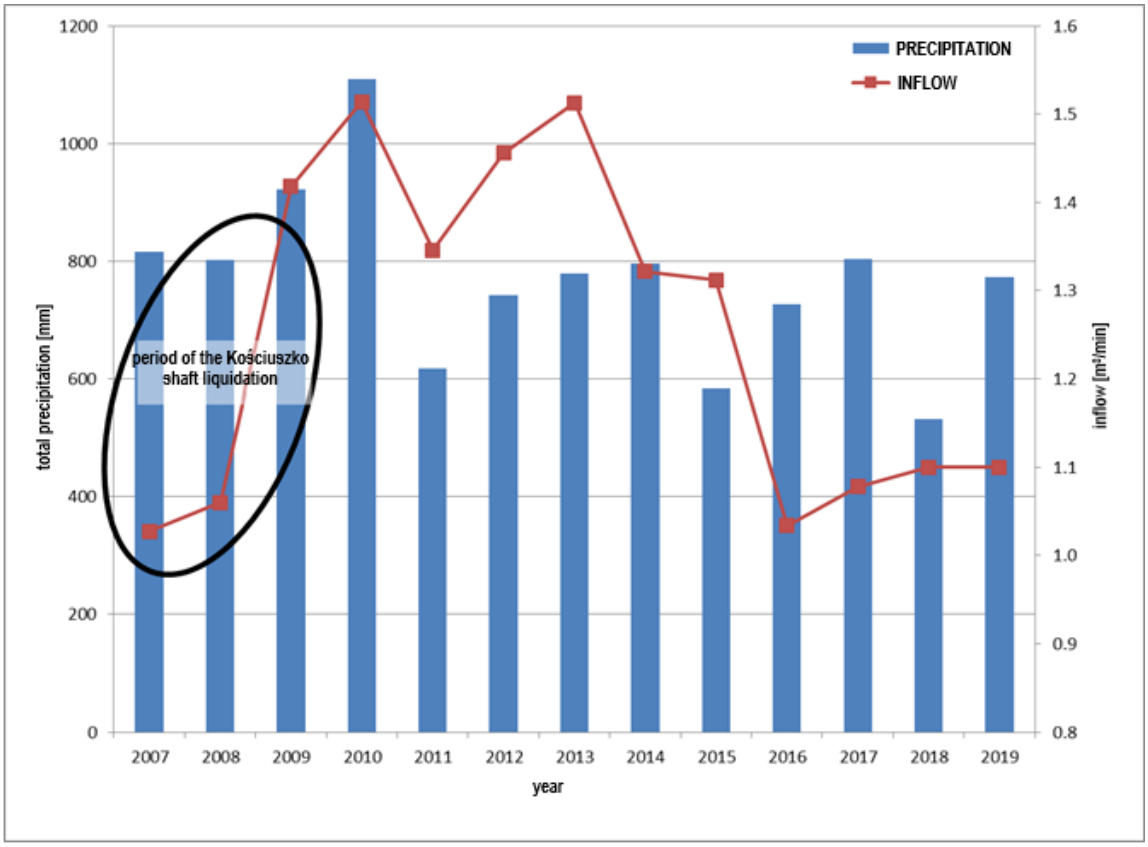

Fig. 1. Variability of the natural inflow of mine water to the "Głowacki" shaft in relation to the variability of the amount of precipitation in the period 2007÷2019 [5]

Comparison of amount of water inflow and the sums of annual precipitation shows that there is no direct relationship between these values. Lack of impact of the amount of precipitation in the years 2016÷2019 is clearly visible, where the amount of precipitation ranges from 531.4 to 804.1 mm (nearly 30%), and the water inflow to the "Głowacki" shaft varies from 1.034 m^3/min to 1,100 m^3/min i.e. approx. 6% (Fig. 1).

In a result of the analysis of mining, geological and surface conditions, but also based on the results of testing and the experience gained from the previously liquidated shafts, the following method of decommissioning the "Głowacki" shaft was decided:

Assumption for the liquidation of "Głowacki" shaft:

- No preparatory work will be carried out in the "Głowacki" shaft in terms of closing the shaft inlets and changes in the shaft's equipment due to the lack of technical possibilities.
- - During liquidation, water flowing to the "Głowacki" shaft will seep through the shaft backfilling to the workings at pos. 600 and further it will flow by gravity to the main drainage system of KWK ROW Ruch "Rydułtowy" mine.
- - If it is not possible to discharge the water inflow through the backfilling in the "Głowacki" shaft, the water at level. 400 will flow through the workings on the level 400, further through the gobs of seam 615/1 to "Blind Shaft III",
- Due to the small cross-section of the shaft and a very large water inflow, very high filtration property for the backfilling material is required. It is assumed that in practice most of the water flowing into the "Głowacki" shaft will seep through the shaft backfilling while the remaining water will flow through the working and gobs to level 400 to " Blind Shaft III".

Publisher: **KOMAG Institute of Mining Technology, Poland**
© 2023 Author(s). This is an open access article licensed under the Creative Commons BY-NC 4.0 (https://creativecommons.org/licenses/by-nc/4.0/)

In the Central Mining Institute, a metallurgical aggregate intended for the liquidation of a mine shaft, fractions of 31.5÷63.0 mm, was tested in a laboratory. Fig. 2 shows grain degradation of metallurgical aggregate before and after discharge into the shaft.

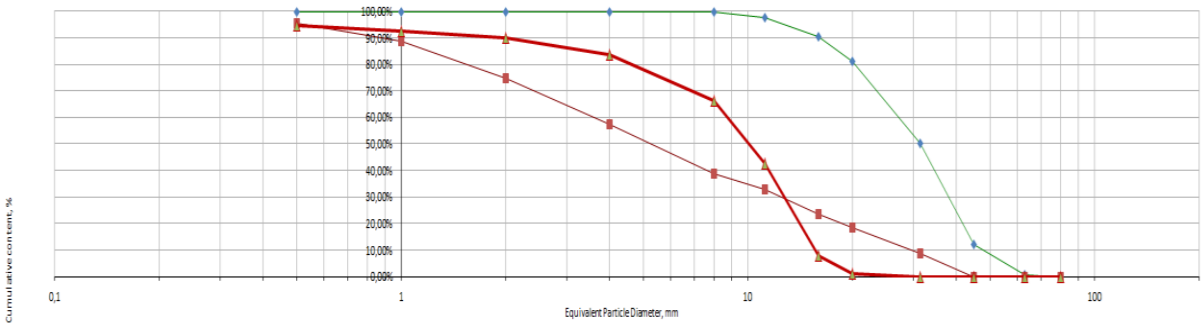

Fig. 2. Grain degradation of metallurgical aggregate 31.5÷63.0 mm before and after discharge into the shaft (green line the material before, red the material after discharge) [5]

The metallurgical aggregate of the following parameters was planned liquidation of the "Głowacki" shaft (Fig. 3÷6):

- grains from 31.5 to 63 mm,
- volume density above 2.0 T/m^3,
- filtration coefficient after discharge to the shaft 1.18*10^{-3} m/s.,
- compressing strength above 100 MPa,
- water-repellent material (Skuty A factor),
- does not adversely affect the chemical composition of mine wate.
- work related to filling the shaft pipe will be carried out from the surface.
- the backfill material will be delivered from the outside by self-dumping vehicles to the storage site and fed from there by a tire loader to a mobile screening machine. From the boom of the mobile screening machine, the charging material will be placed in the shaft through the charging funnel.

The calculated total backfilling volume was 13072 m^3. Implementing the liquidation process based on the presented assumptions, all work of the shaft liquidation was carried out over 3 months. Use of a mobile screening machine before feeding the filling material into the shaft was one of the most important elements, apart from the selection of the right aggregate for backfilling. Based on the experience gained during the liquidation, it was found that despite the fact that the aggregate delivered to the storage yard was of the correct grain size distribution, during the manufacturer's transport from the storage yard to the mobile screen as well as operation of the screen itself, a quite significant amount of bottom product is generated, about 5%. Thanks to the use of appropriate aggregate for liquidation and the use of a mobile screen in the technological process for additional cleaning of the of the backfill material from the bottom product, the shafts were liquidated and water runoff routes were maintained.

Publisher: **KOMAG Institute of Mining Technology, Poland**
© 2023 Author(s). This is an open access article licensed under the Creative Commons BY-NC 4.0 (https://creativecommons.org/licenses/by-nc/4.0/)

Fig. 3. Building of the „Głowacki"shaft landing

Fig. 4. Land development during liquidation

Fig. 5. Position of the screening machine for backfilling

Fig. 6. Discharging chute for liquidation

2.2. Liquidation of "Jas II" and "Jas VI" shafts

The "Jas II" shaft is one of the main shafts, located in the central part of the former mining plant, is a vertical excavation with a depth of 1063 m and a diameter of Ø7.2 m, originally intended for mining, later it served only as an inhalation shaft. "Jas II" shaft was a two-compartment shaft, equipped with a mine shaft hoist with a skip. The run-of-mine was transported in the northern section from a depth of 714 m and the southern section from a depth of 914.5 m. At a depth of 753.6 m, an artificial bottom of the shaft was made, located under the bottom product tank of the northern compartment, with a total height of 10.5 m and a 6-meter shock-absorbing layer.

A reinforced concrete shaft tower with four-rope hoisting machines was built over the shaft. Mining was continued until January 31, 2017, and in 2020 the skip vessels were liquidated. The "Jas II" shaft has a ladder compartment (on the western side between the -400 m and -800 m levels), the following pipelines: fire protection, compressed air, main drainage, supplying technological media, capturing dripping water as well as power cables, shaft signalling and telecommunication cables.

Publisher: **KOMAG Institute of Mining Technology, Poland**
© 2023 Author(s). This is an open access article licensed under the Creative Commons BY-NC 4.0 (https://creativecommons.org/licenses/by-nc/4.0/)

In order to properly fill the shaft pipe of the "Jas II" shaft, the preparation of the backfilling column (Fig. 7) was preceded by disassembling work in the shaft. The scope of these work was as follows:

- shaft gates, platforms, shaft chair covers, protective canopies over inlets at levels -400 m, -600 m and -800 m were disassembled,
- the bottom product tank and the artificial bottom were perforated,
- conveyances, hoisting and balancing ropes were dismantled.

Due to the economic aspect, the main reinforcement girders, guides, pipelines and cabling were neglected during the disassembly of the existing shaft equipment.

The assumptions for liquidation of the "Jas II" shaft determined the technological process, which it was decided in two main stages. In the first stage, the shaft was liquidated by filling it with a self-spreading mineral and cement binder from the sump to the level of 400 m, i.e. in the section where the artificial bottom, ladder compartment, pipelines, etc. were created. At present, the liquidation of the first stage has already been completed. In the second stage, the shaft will be liquidated from the level of 400 m to the shaft core. The technological process will be similar to the one used in the earlier liquidation of the "Jas VI" shaft, with the use of solidified filling mixtures, with near-coal stone aggregate [6].

Basically, in accordance with the project for liquidation of the "Jas II" shaft developed at the Central Mining Institute, the inlets at levels -400 m, -600 m and -800 m were secured by making insulating and resistance plugs. The traffic jams at the levels -400 m and -600 m were located in the working near the shafts. They will consist of two insulating dams spaced at least 6 m apart and a mineral binder with a strength of $R_c^{28} \geq 15$ MPa filling the space between them. The plug securing the level -800 m consists of dams built in the shaft workings and a mineral binder with a strength of Rc28 ≥ 15 MPa filling the shaft from its bottom to the level of -1043 m. of different thickness. Due to the properties of the backfill material and the complete filling of the workings, it was assumed that the dams in the shaft inlets at a given level of the liquidated shaft are to carry the load from the shaft backfill during the material solidification. Thickness of the dams built from the side of the shaft inlets was determined as for single-resistance pyramidal mine water dams.

The use of backfill materials for the liquidation of the shaft with parameters and properties listed in Tables 2 and 3 allows assuming that the reconstruction of the original water conditions in the area of the "Jas-Mos" deposit is not expected. Intake for water inflow to the "Jas II" shaft is planned only in the first stage of forming the backfilling column at the level of -800 m. It is assumed that after the material is set, the backfilling column will not have filtration properties.

Stages I and II were completed after the horizontal workings had been secured with dams and insulating plugs by filling them with binder. The binders were **hydraulic, fine-grained, produced on the basis of high-quality cements**. **The binder in bulk** was transported in closed transport, in airtight road tankers, it was delivered directly from the manufacturer, and after being mixed with water, it was fed through pipelines to each level of the liquidation process [7] (Fig. 8)

Publisher: **KOMAG Institute of Mining Technology, Poland**
© 2023 Author(s). This is an open access article licensed under the Creative Commons BY-NC 4.0 (https://creativecommons.org/licenses/by-nc/4.0/)

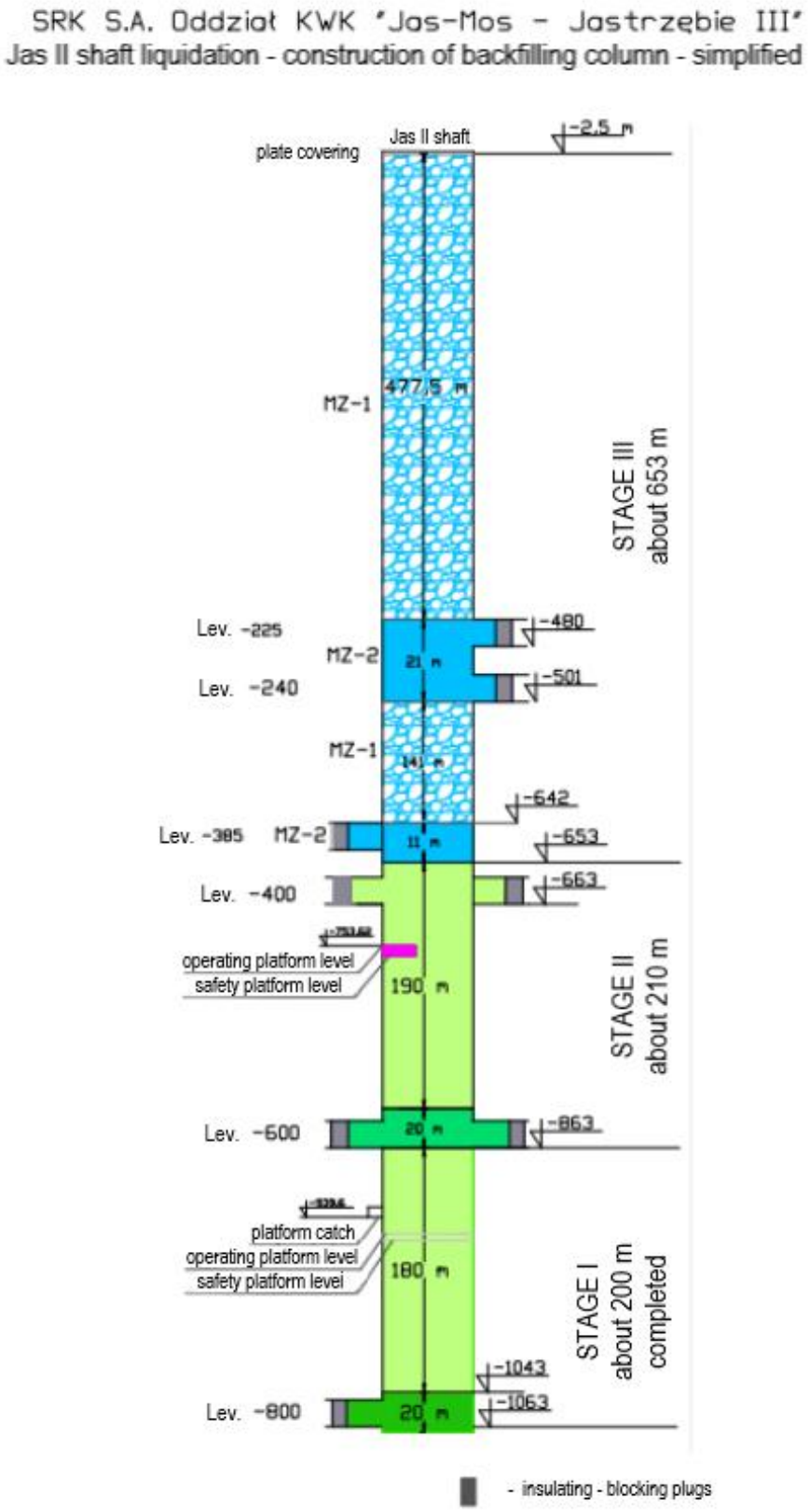

Fig. 7. Schematic diagram of backfilling column for "Jas II" shaft

Publisher: **KOMAG Institute of Mining Technology, Poland**
© 2023 Author(s). This is an open access article licensed under the Creative Commons BY-NC 4.0 (https://creativecommons.org/licenses/by-nc/4.0/)

Table 2. Requirements for the materials used in liquidation of "Jas II" shaft in stages I and II [8]

MZ-3	Fine-grained, self-levelling, hydraulic mineral-cement binder Compressing strength after 28 daysRc28 > 1,5 MPa Flowability acc. to PN-G-11011:1998 > 130 mm Consistency ready-to-be pumped Output > 0,85 m³/Mg
MZ-4	Fine-grained, self-levelling, hydraulic mineral-cement binder Compressing strength after 1 day Rc1 > 1,5 MPa Compressing strength after 28 daysRc28 > 15 MPa Flowability acc. to PN-G-11011:1998 > 130 mm Consistency ready-to-be pumped Output ≥ 1,20 m³/Mg

Fig. 8. Feeding the hydraulic binder with the use of a mixer

Stage III of the shaft liquidation is planned from June 1, 2023. This stage will use 1.0 MPa and 4.5 MPa mixtures. Production of mixtures from post-mining aggregate with grain size below 63 mm and a hydraulic binder will take place on site, i.e. in the area of the shaft landing. Mixtures will be produced using a mixing device. Aggregate from near-coal shale will be delivered from unburnt heaps or directly from the production from processing plants by trucks, while the hydraulic binder will be delivered by tankers unloaded to the silo of the mixing device. Due to the fact that the liquidation of "Jas VI" shaft was completed in April 2023, was carried out using the same technology, the photos in Fig. 9÷12 show characteristic shots of liquidation of this shaft.

Table 3. Project requirements for materials used for the stage III [8]

MZ-1	Solidified filling mix with near-coal stone aggregate Continuously grained mixture for fraction 0-63 mm Compressing strength after 1 day Rc1 > 0,5 MPa Compressing strength after 28 days Rc28 > 1,0 MPa Soakability acc. PN-G-11011:1998 < 20% Compressibility acc. PN-G-11010:1993 (after 28 days of seasoning and pressure 15 MPa) < 10%
MZ-2	Solidified filling mix with near-coal stone aggregate Continuously grained mixture for fraction 0-63 mm Compressing strength after 1 day Rc1 > 0,8 MPa Compressing strength after 28 days Rc28 > 4,5 MPa Soakability acc. PN-G-11011:1998 < 15% Compressibility acc. PN-G-11010:1993 (after 28 days of seasoning and pressure 15 MPa) < 5%

Publisher: **KOMAG Institute of Mining Technology, Poland**
© 2023 Author(s). This is an open access article licensed under the Creative Commons BY-NC 4.0 (https://creativecommons.org/licenses/by-nc/4.0/)

Fig. 9. Installation from the feeding side

Fig. 10. Installation of discharging to “Jas VI” shaft

Fig. 11. The mixer controlling panel

Fig. 12. Installation during filling

3. Conclusions

1) Liquidation of the “Leon III” shaft in the “Rydułtowy I” and “Jas VI” shaft in the Ruch “Jas-Mos”, using mixtures of mine stone aggregate and hydraulic binders produced at the liquidation site, gives great certainty as to the quality of the material used due to ongoing monitoring of the liquidation process.
2) The use of mixtures based on mine stone aggregate and hydraulic binder seals the shaft filling very well, what was confirmed by appearance of water above the filling during breaks in liquidation. At the same time, the water collected above the filling was used to bind the supplied backfill material.
3) The shafts liquidated so far with the use of mixtures of mine stone and hydraulic aggregates show very high stability, so far no losses of the backfill material have been found both in the shafts discussed in the article and in the "Chrobry II" shaft of the "Anna" mine, liquidated in 2013.
4) The applied method of liquidation of the "Głowacki" shaft, with the use of post-metallurgical aggregate with strength of Rc 100 MPa and granulation of 31÷63 mm, as well as the use of a mobile screening machine directly in the shaft landing, ensures high certainty of stable water conditions of the liquidated shafts.
5) The materials used in liquidation of mine workings are the materials processed from waste of other technological processes. The use of this type of materials in place of the often used natural

Publisher: **KOMAG Institute of Mining Technology, Poland**
© 2023 Author(s). This is an open access article licensed under the Creative Commons BY-NC 4.0 (https://creativecommons.org/licenses/by-nc/4.0/)

aggregates, such as dolomite, granite or basalt, is a pro-ecological activity that supports the sustainable development.

References

[1] Technical project of liquidation of the "Leon III" shaft – GIG, Poland

[2] Smoliło J., Chmiela A.: A liquidation of the mine in SRK SA in a processive approach. Zeszyty Naukowe. Organizacja i Zarządzanie, Politechnika Śląska, 2021

[3] Bukowski P., Niedbalska K.: The analysis of selected properties of solid rock materials designed for shafts liquidation. International Multidisciplinary Scientific GeoConference: SGEM, 2013, 2: 467

[4] Prusek S., Całus Moszko J., Bukowski P.: Laboratory tests of filtration coefficient of selected materials used in liquidating shafts in collieries. Journal of Mining Science, 2014, 50: 265-276

[5] Technical project of liquidation of the "Głowacki" shaft – GIG, Poland

[6] Annex to the project of liquidation of the "Jas VI" shaft for SRK S.A. Bytom, Division in Jastrzębie-Zdrój, KWK "Jas-Mos-Rydułtowy I" Ruch Jas-Mos"- GIG, Poland

[7] Pierzyna P.: Liquidation of shafts' workings with the use of the mobile installation. In: IOP Conference Series: Earth and Environmental Science. IOP Publishing, 2018. p. 012011

[8] Technical project of liquidation of the "Jas II" shaft with the investor's cost estimate - update – GIG, Poland

Publisher: **KOMAG Institute of Mining Technology, Poland**
© 2023 Author(s). This is an open access article licensed under the Creative Commons BY-NC 4.0 (https://creativecommons.org/licenses/by-nc/4.0/)

https://doi.org/10.32056/KOMAG2023.3.4

Technical and technological support of the technology of activating the process of gasification of thin coal seams

Received: 22.09.2023

Accepted: 30.10.2023

Published online: 31.10.2023

Author's affiliations and addresses:

[1] Dnipro University of Technology, 19 Yavornytskoho Ave., 49005, Dnipro, Ukraine

Volodymyr FALSHTYNSKYI [1], Andrii PERERVA [1], Vladyslav CHALYI [1], Vladyslav PSYUK [1], Roman DYCHKOVSKYI [1*]

*** Correspondence:**

e-mail: Dychkovskyi.r.o@nmu.one

tel.: +38 098 523 33 06

Abstract:

According to the tests results of the technology of reverse jet flow, to balance the geometric and physical parameters of the active zones of the reaction channel of the underground gas generator during the gasification of low-power coal seams. The parameters of activation of the oxidizing and reducing zones of the fire blowout were established, taking into account the outgassing of the coal seam in space and time, the impact of mining and geological parameters as well as geotechnical and thermochemical processes, securing the even advance of the fire blowout along the length of the reaction channel of the underground gas generator. It was established that the intensification of the gasification process of thin and ultrafine coal seams increases the quantitative and qualitative parameters of exothermic and endothermic reactions, which have an impact on increasing the efficiency of the underground georeactor and determines the quality parameters of the gasification product.

Keywords: experimental bench plant, model of the gasification process, underground gas generator, reaction channel, fire break, low-power coal seams, reverse mode

Publisher: **KOMAG Institute of Mining Technology, Poland**
© 2023 Author(s). This is an open access article licensed under the Creative Commons BY-NC 4.0 (https://creativecommons.org/licenses/by-nc/4.0/)

1. Introduction

The technical and technological support of the process of underground gasification of coal includes a set of measures and equipment necessary for the effective implementation of this process. Underground coal gasification is the process of converting coal seams into high-calorific gas, which can be used for the production of electricity, heat, synthesis of various chemical products and fuel gases [1-3].

The main components of the technical and technological support of the process of underground gasification of coal are the following:

- Mine infrastructure. This includes construction and maintenance of mines for opening the coal seams. Mines that involve the synthesis technology within one facility must be equipped with special systems of ventilation, safety and monitoring of working conditions [1, 4];
- Gasification plant. This is the main equipment used to convert coal into gas. This installation includes a gasification channel, where chemical reactions take place, and systems for supplying gaseous mixtures and removing the gasification products [2, 5, 6];
- Gas purification and treatment systems. The resulting gas contains a certain amount of impurities that must be removed before its use. Gas cleaning and processing systems include filters, condensing units and other equipment for cleaning and preparing gas to be a commercial product [5, 7];
- System of transportation and accumulation. Cyclic or continuous flow systems are used to transport the prepared technical gas. This may include special piping systems, tanks and gas storage tanks [5, 8];
- Energy supply and automation systems. Appropriate power supply, automation and control systems are used to secure proper management of the gasification process and to monitor operating parameters [5, 9];
- Safety and environmental systems. Ensuring the safety of workers and the environment is a major aspect of underground gasification. This system includes a ventilation network, safety sensors, gas control systems and other measures [10].

Due to the complexity and potential risks of underground coal gasification, effective technical and technological support is important to ensure the successful implementation of this process and minimize negative impacts on the environment. During the gasification of thin coal seams, significant heat losses are observed in the rock of the roof and floor, which significantly affects the output of the gas generator during the production mode of the gasification process [10, 11]. In the production mode, there is an increase in the speed of the fire in the oxidizing zone and an increase in the length of the reaction channel, which leads to an imbalance between exothermic processes in the oxidizing zone and endothermic processes in the reducing zone, negatively affecting the performance of the underground coal gas generator [12]. Reverse operation aims at activating the thermochemical processes of coal gasification, relevant at the first stages of putting the underground gas generator into operation, as well as at the end of the work [13]. When operation of the underground gas generator is stopped, destabilization of the gasification process of the coal seam leads to a decrease in leak tightness coefficient of the georeactor, which significantly affects the parameters of the coal seam gasification due to the loss of coal and generator gases as well as blowing [4].

Establishing the rational technological parameters for reversing the active zones of the reaction channel of the underground gas generator is especially relevant in the regimes of ignition of a thin seam, the transition to the gasification regime, and in the process of extinguishing in thermochemical processing and mining of a coal seam.

2. Materials and Methods

Research work on implementation of reverse technology in the gasification of low-power coal seams were developed at the "Pidzemgaz" plants in gasification of thin hard coal seams in the conditions of Donbas region, but the designs of underground gas generators and technological innovations of that time did not allow testing and implementation of reverse technologies.

Publisher: **KOMAG Institute of Mining Technology, Poland**
© 2023 Author(s). This is an open access article licensed under the Creative Commons BY-NC 4.0 (https://creativecommons.org/licenses/by-nc/4.0/)

Gained Ukrainian and foreign experience in designing and operation of industrial and experimental underground gas generators allowed scientists of the Dnipro Polytechnic National Technical University to develop new designs of underground gas generators and technologies for activating the gasification process of low-power coal seams with adaptation to complex mining and geological conditions [2].

New technological solutions increasing the reliability and efficiency of the gasification process of thin coal seams were developed by modelling the rock-coal seam, the coal seam and the construction of the underground gas generator on experimental installations according to the criteria of similarity [14].

According to the information of operating underground gas generators, bench and laboratory tests and analyses of parameters of the technology of reversing the active zones of the reaction channel of an underground gas generator, it was established that the main reasons for the unstable operation of underground low-power gas generators during gasification of coal seams є [15] are the following:

- heat loss during the active heat exchange of the fiery blowout of the coal seam with the rocks in it;
- non-uniformity of the advance of the fire exit from the reaction channel of the gas generator due to the higher advance of the oxidizing zone;
- losses of dust mixtures, generator gas and coal when the gas generator space increases and the appropriate tightness of the underground gas generator changes.

In today realities, the most available methods of testing the parameters of the technology of intensification of the process of gasification of low-power coal by reversing the active zones of the reaction channel of the underground gas generator of formations, taking into account the impact of mining and geological conditions, are the analysis of experience in the gasification of thin coal seams, bench tests and methods of mathematical and computer modelling with application of software packages such as MTBalance SPGU, "Devices Systems", Monitor QB. and "GeoDenamics Lite" [12].

Modelling and testing the coal gasification processes in underground boreholes was carried out on the ESU, designed and patented at the Dniprovska Polytechnic National Technical University [16]. The coal seam, structures of the underground gas generator, rock stratum and coal gasification processes were created according to the criteria of the similarity and suitability of the coal seam to the LNG. Assembly, preparation and testing the SPGV in ESU were performed on industrial sites with the financial and technical support of DTEK "Pavlogradvugilya", the company "Donetskstal" and the Ministry of Science and Education of Ukraine (Fig. 1).

One of the points of testing was establishing the rational parameters of the t reverse operation for activation of fire breakout zones in the conditions of an increase in the gassed space, changes in the tightness and length of the reaction channel of the underground gas generator, taking into account space and time.

Publisher: **KOMAG Institute of Mining Technology, Poland**
© 2023 Author(s). This is an open access article licensed under the Creative Commons BY-NC 4.0 (https://creativecommons.org/licenses/by-nc/4.0/)

Fig. 1. Assembly, preparation and testing the SPGV in ESU: 1 – transitional cooling box; 2 – condensate tank; 3 – generator gas cooling tank; 4 – a container for collecting condensate; 5 – gas outlet pipeline; 6 – IRVIS sensor; 7 – configurator for cleaning generator gas from hydrogen sulphide (H2S); 8 – chimney; 9 – transition pipe; 10 – vertical gas outlet pipe; 11 – section No. 1, testing and measuring complex (thermocouples): display of temperature sensors (thermocouples), TERA "Devices System" software based on the Firebird 2.1 database; 12 – reserve compressor; 13 – main compressor; 14 – steam generator; 15 – section No. 2, system for controlling quantitative parameters of generator gas blowing and pressure: IRVIS - K300, gas analysers Garboards 3200L and BX-170. The change in displacement of the roof rocks, as the gasification area of the gas generator increases, was provided by the database of reference sensors and the Monitor QB program; 16 – formation of a solid coal together with the installation of reference sensors

3. Results

3.1. Formation of the gas generator system and its start-up

Ignition of a coal seam, fire treatment and creation of a reaction channel, during the experiment, was secured by reversing the stream flows with the optimization of the material-heat balance of the thermochemical process during the transition from burning to gasification of coal in the seam with formation of adaptive parameters of the oxidation and reduction zone and stabilization of the auto thermality of the LNG process during balancing exothermic and endothermic reactions.

Publisher: **KOMAG Institute of Mining Technology, Poland**
© 2023 Author(s). This is an open access article licensed under the Creative Commons BY-NC 4.0 (https://creativecommons.org/licenses/by-nc/4.0/)

Control of the gasification process of the thin coal seam model took place from the intake control unit and the blow reverser. Part of the air blast was fed through the blast well, and the active part of the blast mixture (oxygen, steam) was fed through a flexible pipeline directly to the fire outlet in the oxidation zone of the reaction channel, where exothermic processes generating heat, ensures activation of endothermic processes in the reduction zone, forming the balance of physical rates and kinetics of thermochemical reactions.

The coal seam was ignited through the ignition hole of the test stand (Fig. 2, a) d = 100 mm with the help of red-hot pieces of coal and the blowing of air enriched with oxygen (O_2 = 28÷40%, with a consumption of Q = 1.8÷3 m^3/min). The ignition temperature of the G-grade coal seam and pressure were recorded using a pyrometer, pressure sensors, and thermocouples and were in the range of T = 405÷538°C, at a pressure of p = 0.14÷0.2 MPa. The direction of the blow-through of the channel between the blowhole and the gas-discharge well coincided with the direction of the blow and was in the temperature range of T = 584÷705°C with a pressure of p = 0.25÷0.36 MPa, while the speed of the blow-through of the channel was V_k = 0.7÷0 .96 m/h. According to the testing method, the initial stage of the blow-through of the reaction channel of the gas generator was carried out in the blowing mode, shift to the combined mode "compressor - flue draft" made it possible to reduce the pressure p = 0.14÷0.3 MPa and increase the speed of the blow-through V_k = 1÷1.3 m/h. Formation of active zones and thermal intensification of the reaction channel of the gas generator model was provided by the reverse flow of the blast from the blast and gas discharge wells to the fire hole in the temperature range T = 695÷1004°C with a pressure of p = 0.2÷0.28 MPa, which made it possible to form an oxidizing, transitional and the recovery zones of the gas generator. Length of the oxidation zone was 27÷33% the reaction channel, the transition zone was 0.4÷0.7%, the reduction zone was the length of the remaining reaction channel.

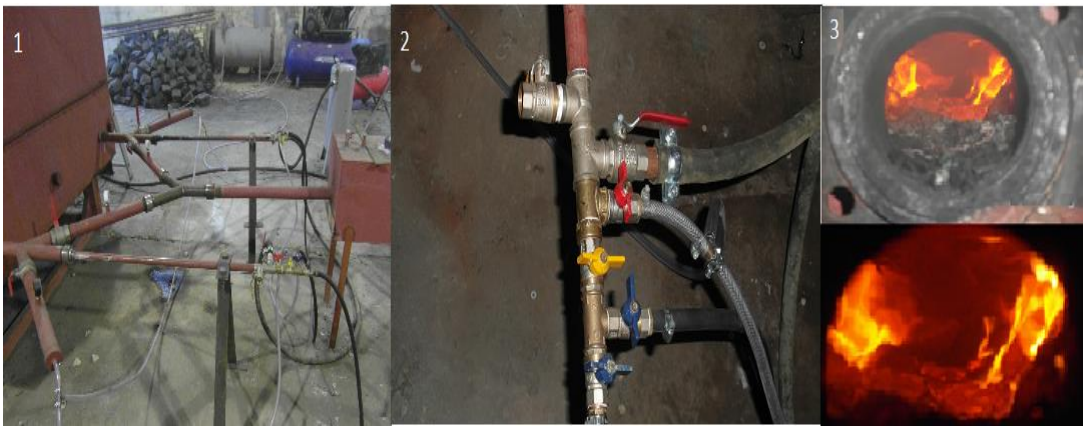

Fig. 2. The coal seam ignition process and the thermal treatment of the reaction channel of the underground gas generator model: 1 – connection of the unit for the integration of the supply and discharge of blast mixtures and generator gas with the gas generator stand: 2 – the control system for blast supply modes and reverse operations; 3 – visualization of the activation of oxidation and reduction zones when applying reverse streams

Reversing the dust mixtures and control of supply and pressure regimes during ignition and formation of the reaction channel allowed after 3 hours bring the gas generator into stable gasification mode. After 3 hours 40 minutes of the test, at 0.2 m from the point of the blast supply in the oxidation zone of the reaction channel, the temperature in the range T=590÷685°C was recorded by a pyrometer. At 0.76 m from the point of blowing, the temperature reached T=884÷1007°C, the oxygen content did not exceed 1.5%, and the carbon dioxide content reached 12.6%.

Temperature of the roof rocks after 5 hours and 35 minutes of heating, above the fire hole at 0.1 m from the point of the blast was 412÷470°C, at 0.62 m – 566÷734°C, at 0.87 cm – 664÷750°C, at 1.18 m – 450÷529°C. The generator gas output was 2.1÷2.4 m^3/min, with an average water content of 182.5 g/cm^3 and with a lower combustion temperature in the range of 2.5-7.2 MJ/m^3.

Publisher: **KOMAG Institute of Mining Technology, Poland**
© 2023 Author(s). This is an open access article licensed under the Creative Commons BY-NC 4.0 (https://creativecommons.org/licenses/by-nc/4.0/)

Increase of the degassed space of the gas generator by the dimensions $S_{v.p.}$ = 0.12÷3.86 m^2 and the change in tightness of the gas generator were observed, depending on the degree of coal gasification in the seam, as well as the increase in the length of the oxidation zone and the reaction channel, associated with the displacement of the roof rock layers, the growth of vertical and horizontal fracturing, and the difference in the speed of advance of the active zones of the gas generator. At the tenth hour of the test, destabilization of the gasification processes was recorded: changing in the temperature regime and pressure along the reaction channel, a change in the quantitative and qualitative composition of the generator gas, which is associated with increase of ballast gases and a decrease in calorific value.

Application of the reverse technology of the active zones of the reaction channel in the underground gas generator, variations in the modes of supply by blowing pressure made it possible to align the line of the fire gap, to restore the appropriate length of the reaction channel, and also to stabilize the quality indicators of the generator gas. Thanks to the reverse technology, the coal seam gasification process was maintained for 5 hours and 30 min at the damping stage, according to the method of the experiment and the stable transition from gasification to the mode of damping the work.

Parameters of the fuel components of the generator gas during the bench test on the gasification of a low-power coal seam are shown in Fig. 3.

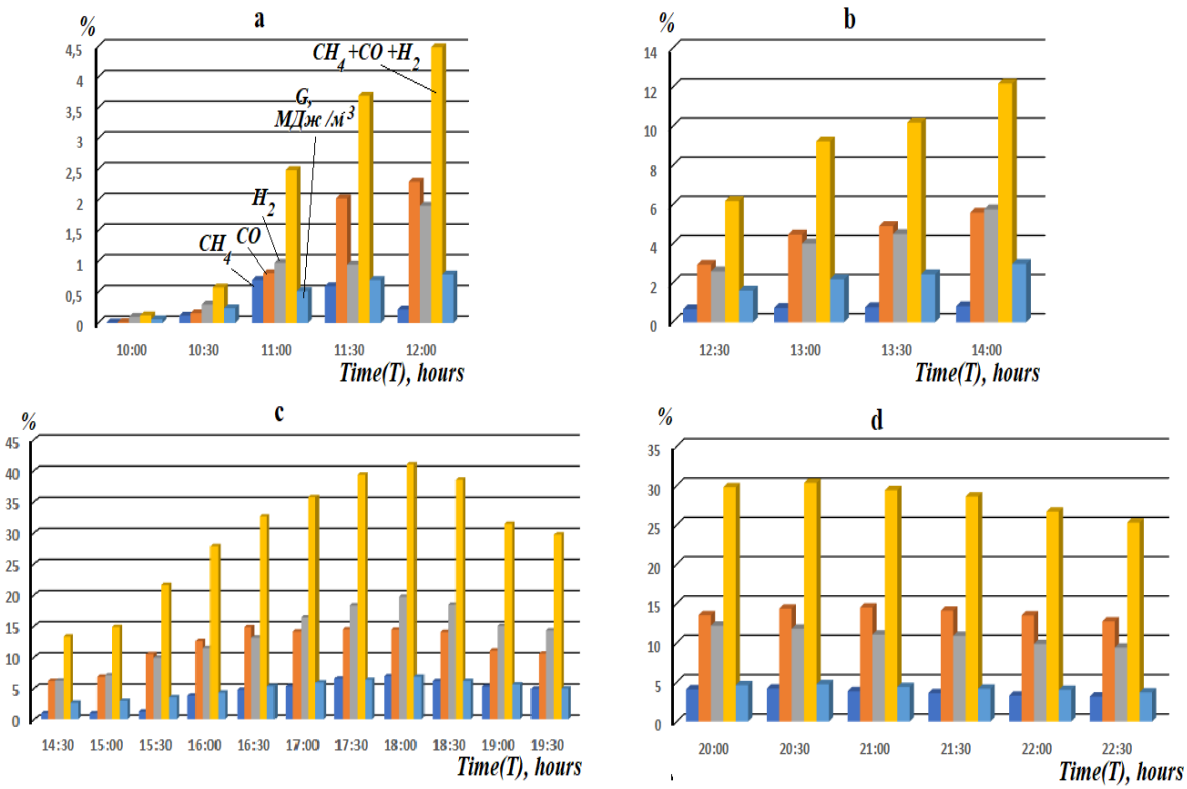

Fig. 3. Parameters of the fuel components of the generator gas during the bench test on the gasification of a low-power coal seam: a – mode of ignition, burn-through and formation of the reaction channel; b - mode of reverse works for the formation of active zones of the reaction channel of the underground gas generator; c – mode of productive, balanced gasification of a thin coal seam; d – mode of reverse operations maintaining the proper parameters of gasification in a view of increasing the gasified space and the loss of required tightness by the gas generator during stopping the work on gasification of a thin coal seam

When using reverse operations on the side of the recovery zone of the reaction channel of the gas generator, the following is provided: no blast mode, removal of generator gas through the blast well in a exhaust gases pipe, supply of oxygen-enriched blast (O_2 = 35÷62%) through a flexible control pipeline

Publisher: **KOMAG Institute of Mining Technology, Poland**
© 2023 Author(s). This is an open access article licensed under the Creative Commons BY-NC 4.0 (https://creativecommons.org/licenses/by-nc/4.0/)

directly to the fire outlet, as well as steam-air blast along the gas borehole. During the bench test, after 58 min changes in temperature and productive parameters along the length of the zone were recorded, an increase in the heat capacity C, kJ/(kg K) and a decrease in the thermal conductivity λ, W/(m K) of the gas condensate of oxidation processes containing rocks. The pressure during reverse operations was in the range of 0.45-0.6 MPa at the beginning of operations, while the oxidation processes was stabilized the pressure was 0.18-0.22 MPa.

Fig. 4 presents the results from testing the parameters of reverse operation during the underground gasification of a low-power coal seam in the real conditions, taking into account mining and geological, technological and geo-mechanical parameters as well as the thermochemical process of gassing the coal seam of the SPGV site.

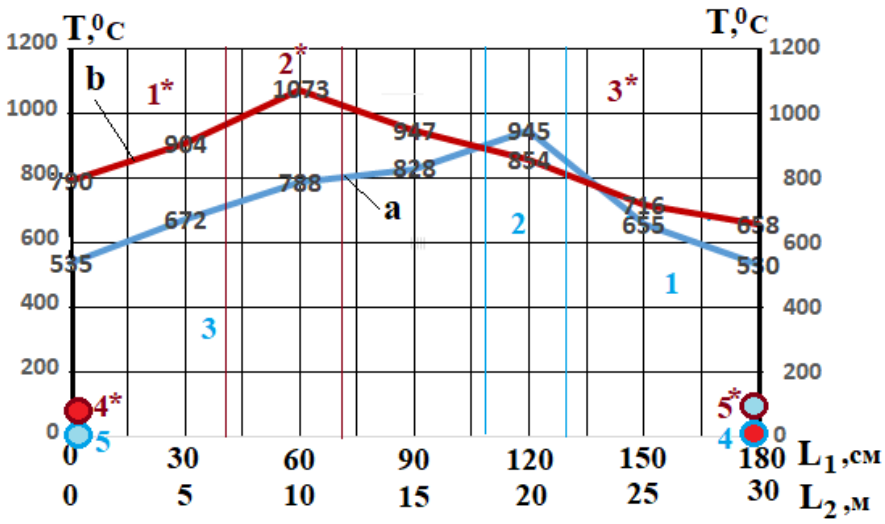

Fig. 4. Temperature and technological parameters of reverse operations during the bench test on underground gasification of a low-power coal seam: 1 – temperature distribution before the reverse (initial stage of process damping), 2 – temperature distribution after the reverse (the process of a stable gasification regime), 4 - oxidizing zone, 5 - transition zone, 6 - reducing zone, 7 - jet borehole (stable gasification process), 8 - gas removal borehole (stable gasification process)

3.2. Analyses of the technological parameters of reverse operations during underground gasification of a low-power coal seam.

Calculation of displacement of the oxidation and reduction zone of the reaction channel of the underground gas generator is based on the results of mine tests, bench tests and data on the material balance of the underground coal gasification process.

According to analysis, the quantitative parameters of coal gasification in the oxidation zone of the reaction channel of the underground gas generator are determined using the following formula:

$$A_{\text{окz.}} = \frac{Q_{okz}}{n}, \text{ t/h} \quad (1)$$

where:

Q_{okz} – gas production by the oxidation zone, m^3/h,

n – the volume of generator gas per one kg of coal, 2 m^3/kg,

in the regeneration zone:

$$A_{v.z} = \frac{Q_{v.z.}}{n}, \text{ t/h} \quad (2)$$

where:

$Q_{g/g}$ – generator gas output from the gas generator, m^3/h;

$Q_{v.z}$ - production of gas by reduction, $Q_{v.z} = Q_{g/h} - Q_{ok.z}$, t/h.

Publisher: **KOMAG Institute of Mining Technology, Poland**
© 2023 Author(s). This is an open access article licensed under the Creative Commons BY-NC 4.0 (https://creativecommons.org/licenses/by-nc/4.0/)

After determining the parameters of coal outgassing in the active zones of the reaction channel, the speed of advance of the generator gas escape was justified:

$G_{v.d.}$ – the amount of coal gasified per day, $Q_{ok.z}+Q_{v.z}\cdot T_g$, t/day; $G_{v.1p.m}$ - amount of coal in 1m.p. fire impact, $G_{v.1p.m.}=l_{r.k.}\cdot 1\cdot m\cdot\gamma$, t/1p.m:

– advance of fire escape of the underground gas generator

$$V_{v.v}=\frac{G_{v.d.}}{G_{v.1p.m.}},\ \text{m/day} \tag{3}$$

– advance of the fire gap of the recovery zone of the reaction channel

$$A_{v.z.day}=A_{v.z.day}\cdot T_G,\ \text{t/day};\ V_{v.z.day}=\frac{A_{v.z.day}}{G_{v.1p.m.}},\ \text{m/day} \tag{4}$$

– difference between the advance of gaps in the oxidizing zone and in the reducing reaction channel of the underground gas generator

$$V_{ok.z}=V_{v.v.}-V_{v.z.},\ \text{m/day} \tag{5}$$

According to the calculation (Fig. 5), the increase in the length of the reaction channel of the underground gas generator is determined, taking into account the difference in the advance of the active zones.

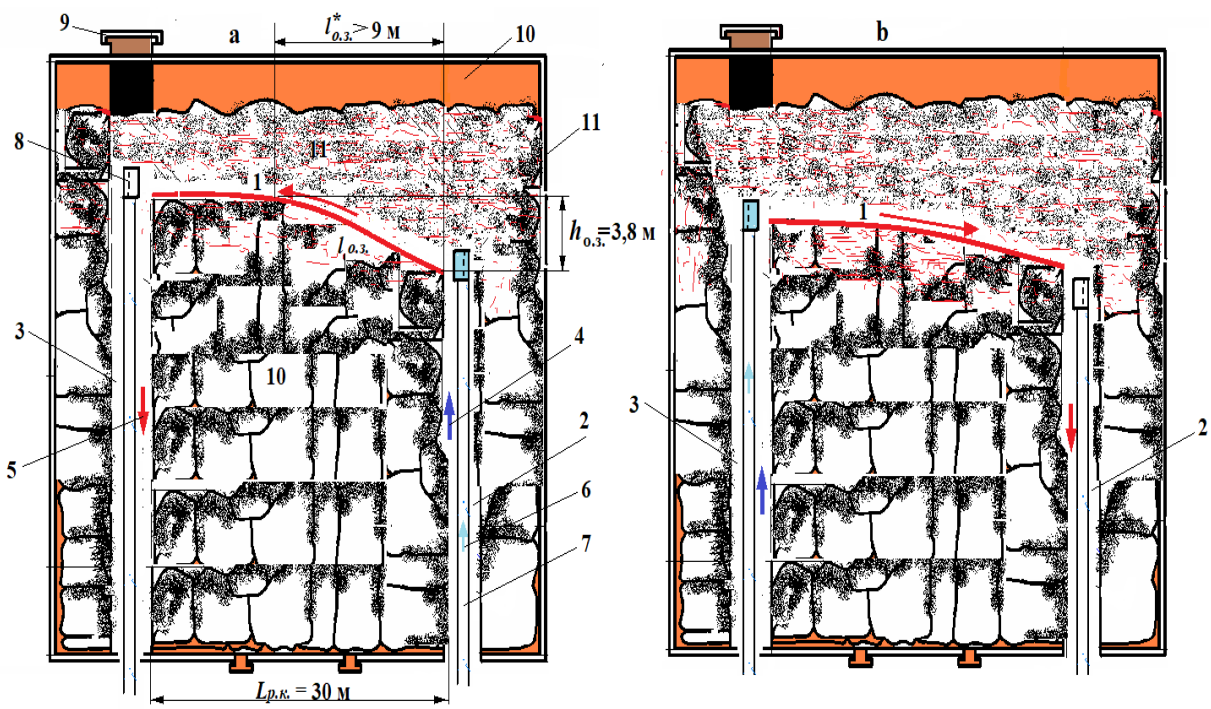

Publisher: **KOMAG Institute of Mining Technology, Poland**
© 2023 Author(s). This is an open access article licensed under the Creative Commons BY-NC 4.0 (https://creativecommons.org/licenses/by-nc/4.0/)

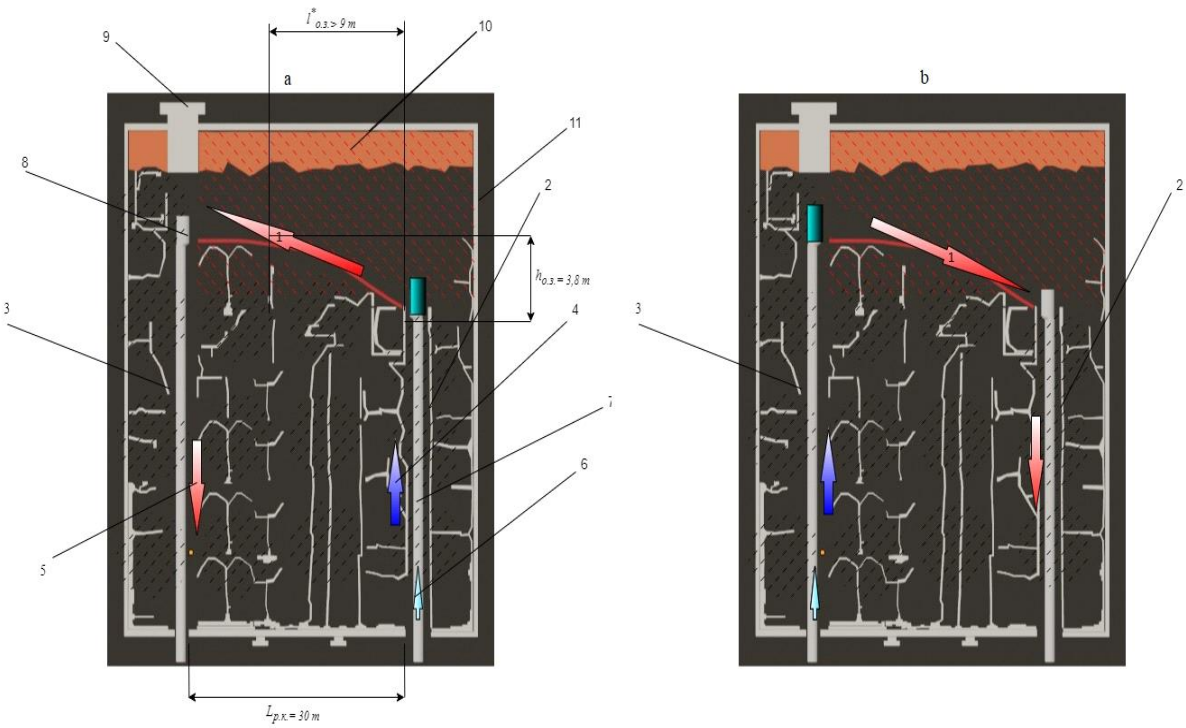

Fig. 5. Scheme for calculating the onset of reverse work according to the main technological parameter - the length of the oxidation zone of the reaction channel: a – conditions for the onset of reverse work; 1 – reaction channel of the gas generator, 2 – blow borehole, 3 – gas discharge borehole, 4 – air blowing, 5 – generator of gases, 6 – oxygen-enriched blowing, 7 – controlled flexible pipeline, 8 – heat-resistant perforated nozzle, 9 – coal bed ignition nozzle , 10 – thermal insulation, 11 – degassed space of the gas generator; b –reverse operation to activate the zones of the gas generator reaction channel

Increase in the length of $\mathbf{L_{r.k.}}$ and oxidation zone $\mathbf{l_{o.z.}}$, the reduction or absence of the transition zone and the reduction of the reduction zone of the reaction channel due to the increase in the speed of the flame discharge of the oxidation zone, which affects the balance of the gasification process is the reason for starting the reverse operation:

$$l_{o.z.} = \sqrt{{l^*_{o.z.}}^2 + {h_{o.z}}^2}, \text{ м} \tag{6}$$

$$l_{v.z.} = L_{r.k.} - l_{o.z}, \text{ м} \tag{7}$$

where:

$l^*_{o.z.}$ – length of the oxidation zone of the reaction channel in the underground gas generator 9 м,

$l_{v.z..}$ – regeneration zone, m.

An increase in the length of the oxidation zone by 30% or more leads to an imbalance in the generation and transfer of thermal energy for thermochemical reactions in the reduction zone of the gas generator. Under these conditions, it is assumed that reverse operations ensure the linearity of the fire gap and activate the gasification processes, creating conditions for the balance of the active zones of the reaction channel of the gas generator. The results of bench and analytical tests on implementation of reverse operations during the gasification of low-power hard coal seam C6, grade DH, Solinovsk coal basin, Pokrovsky district, with a capacity of m=0.7-0.75 m, are presented in Fig. 6.

Publisher: **KOMAG Institute of Mining Technology, Poland**
© 2023 Author(s). This is an open access article licensed under the Creative Commons BY-NC 4.0 (https://creativecommons.org/licenses/by-nc/4.0/)

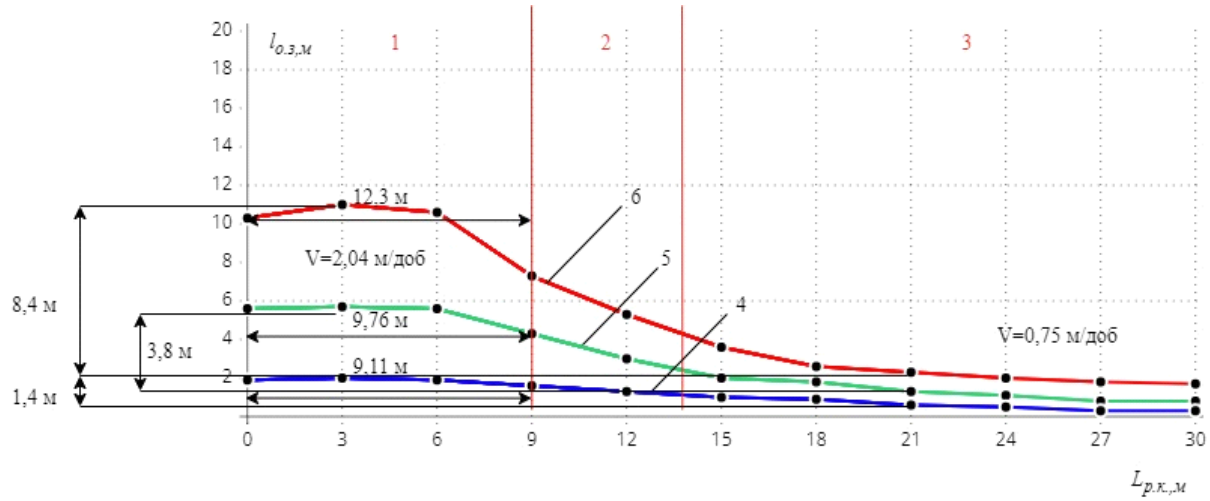

Fig. 6. Impact of the parameters of the reaction channel zones movement in the underground gas generator on the conditions of the onset of reverse operation, taking into account geological conditions, technical indicators and geo-mechanical parameters: 1 - oxidizing zone, 2 - transition zone, 3 - reducing zone, 4 - 1 day, 5 - 2 days , 6 - 3 days; 1.4, 3.8, 8.4 m – increase of the parameters of advance of length of the oxidizing zone after fire breaks out, relative to the length of the reducing zone; 9.11, 10.16, 12.3 m - increase in the length of the oxidation zone, according to the difference in the speed of the active zones of the gas generator

Balancing the thermochemical processes, geometrical and temperature parameters as well as directionality of gasification of the coal seam during reverse operations, ensured the formation of active zones of the reaction channel of the gas generator in 1.2 - 1.35 hours. According to the results of the temperature range, the energy balance of the reaction channel and the composition of the generator gas, during the bench tests and analyses, it should be stated that the recovery and stability of the gasification process has been achieved in the short time from starting the reverse work [15].

3.3. Chemistry of the reverse operations during underground gasification of a thin coal seam

Among the gasification processes, there are autothermal ones, in which the heat required for the endothermic gasification process is obtained from burning part of the injected fuel, and autothermal ones, in which the required heat is supplied from the outside using a solid or gaseous medium. In practice, these processes are used in combination - multi-stage gasification. The coal gasification process is associated with the reactions given in Table 1.

Table 1. The main chemical reactions of the gasification process

Reaction	ΔH, kJ/mole
$C + O_2 = CO_2$	– 393,7
$C + 0{,}5O_2 = CO$	– 109,4
$C + CO_2 = 2\ CO$	+ 172,5
$C + H_2O = CO+H_2$	+ 131,4
$C + 2H_2O = CO_2+ 2H_2$	– 41,1
$C + 2H_2 = CH_4$	– 74,8
$CO + 3H_2 = CH_4+H_2O$	– 206,2
$2CO + 2H_2 = CH_4+CO_2$	– 123,8

Publisher: **KOMAG Institute of Mining Technology, Poland**
© 2023 Author(s). This is an open access article licensed under the Creative Commons BY-NC 4.0 (https://creativecommons.org/licenses/by-nc/4.0/)

It should be noted that the thermodynamic basis of the coal gasification process has been investigated, but their kinematics has not been sufficiently explained.

Depending on a way using the generator gas, such conditions are applied in which a gas-condensate mixture of the required composition is obtained.

Realities of the fuel and energy complex of Ukraine have a significant need for hydrogen, synthesis gas, reducing gases for the gasification of solid fuels and, first of all, from balance reserves, cut and crushed coal, thin and ultra-thin coal seams. Generator gas is processed as a chemical raw material, therefore the content of carbon dioxide (CO_2) and nitrogen (N_2) in its composition should be minimal, therefore the advantage in the thermochemical gasification of solid fuel under pressure when using oxygen (steam-oxygen blowing mixtures).

For various chemical reactions, the mixtures of CO with H_2 of different ratios are used. For example, for the synthesis of methanol or aliphatic hydrocarbons, a gas with a ratio of $CO:H_2=1:2$ is used, and when aldehydes are obtained by the hydroformylation reaction (oxosynthesis), a synthesis gas with a ratio of $CO:H_2=1:1$, which reacts with olefins, is used. For the synthesis of methane the ratio $CO:H_2$ should be 3:1.

Changing the composition of the generator gas during gasification, regarding the CO and H_2, is possible by processing it using the following conversion process:

- catalytic conversion of carbon monoxide (to increase the hydrogen content);
- catalytic conversion of methane (to increase the synthesis gas content);
- scrubbing from carbon dioxide (to increase the oxidant content).

Depending on the conditions of the gasification process, it is possible to change the composition of the obtained gas, for example, to increasing the content of carbon monoxide in the gas is possible by increasing the reaction temperature. The power of the gas generator is determined by many parameters (pressure, temperature, composition of dust mixtures, contact time). This process is carried out in three main ways: in a stationary mode, in a fluidized bed and in a flow of pulverized fuel. Also the method of well underground gasification (SGU) on moving nozzles and an activator [15] has been developed as well as gasification in the environment of molten coolants (ash, salt, metals). Plasma gasification of pulverized fuel, during which the oxidizer is heated to high temperatures, enables intensification of the coal gasification process.

It is possible to increase the efficiency of the reaction in the process due to the reverse chemical transport [16]. The reverse process was modelled on the basis of a chemical system consisting of a cylindrical tube placed in a furnace with a constant temperature (Fig. 7).

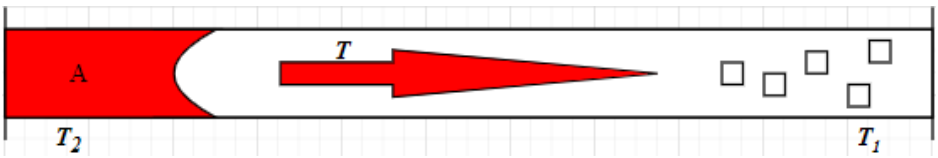

Fig. 7. Chemical transport in a cylindrical tube. Transport from the zone with temperature T2 to the zone with temperature T1

The basic principles of chemical transport can be demonstrated when transport reactions take place in a cylindrical tube with a different temperature between its ends, using the following equation:

$$A\ (solid) + B\ (gas) = AB\ (gas),$$

$$n_{AB} = (Dqt/sRT)(P_{AB(2)} - P_{ABm}),$$

where n_{AB} is the number of moles of substance AB that diffused, D is the diffusion coefficient, q is the cross section of the tube, s is the length of the diffusion path, t is

Publisher: **KOMAG Institute of Mining Technology, Poland**
© 2023 Author(s). This is an open access article licensed under the Creative Commons BY-NC 4.0 (https://creativecommons.org/licenses/by-nc/4.0/)

the process duration, R is the gas constant, T is the absolute temperature along the diffusion path, $P_{AB(i)}$ is proportional to the pressure of component *AB* at the point with temperature T_1.

In the right-hand side of the expression for pAB, the first factor reflects the gas displacement and the apparatus constant, and the second factor reflects the heterogeneous reaction. In this case $\mathbf{T_2>T_1}$.

If a solid substance A reacts with a gaseous substance B to form a gaseous compound AB, and if this reaction is reversed, then chemical transport can occur. If the observed reaction is endothermic, the solid substance A will decompose at higher temperatures T2 with the formation of a gaseous compound AB, while after the migration of AB to the point with temperature T1, the reverse reaction occurs and component A is deposited from the gas phase. In the case of exothermic reactions proceeding in the same temperature gradient, part of the substance is moved in the reverse direction $T_1 \rightarrow T_2$.

Diffusion in the gas phase is the stage that determines the rate of the total transport reaction. This means that the concentration gradient necessary for diffusion is determined by the presence of heterogeneous equilibrium at temperatures $\mathbf{T_2}$ **and** $\mathbf{T_1}$.

According to this equation, metals and silicates contained in the rock can be transported in significant quantities through the gas phase at 1200^0 C or at higher temperatures. Further, at lower temperatures, they are deposited in the form of well-formed crystals that serve as catalysts for the reversible process. Exothermic transport reactions have long been known, investigated in the research work of Van Arkel, as well as Van Arkel and de Boer [17]. These studies found wide, practical use in purification of metals.

Concentration gradient caused by the temperature dependence of the heterogeneous equilibrium is the driving force of the process. When selecting the transport reactions, the following factors are of significant importance:

- chemical transport is possible only when gaseous substances participate in the reactions (except for the transfer of solid matter). Only in this case, all components are mobile in the gas phase;
- the reaction must be reversed;
- the equilibrium position of transport reactions should not be sharply shifted either towards the starting substances or towards the gaseous product. Otherwise, the concentration gradient is negligible.

By substituting the real values into the diffusion equations ($q \approx 3$ cm^2, $s \approx 10$ cm), the transfer can be efficient if the factor $\Delta P_{AB}/\Sigma P$ P equals at most 10^{-4}. It follows that not one of the partial pressures that should be taken into account in the transport process cannot be less than the value given by this factor.

Under other constant conditions, the transfer efficiency will be small when the gradient (ΔP_{AB}) will be maximum. In this case, the free energy of the transfer reaction will be near zero. However, these conditions are not necessary.

When the transport reaction is not connected with the next reaction, the necessary concentration gradient in the gas phase is also decisive for the reactions to proceed under isothermal heating conditions (practically). The important terms are described in the following equations:

zone 1: A (solid) + B (gas) = AB (gas) (1)
zone 2: AB (gas) + C (solid) = AC (solid) + B (gas); (2)
totally: A (solid) + C (solid) = AC (solid). (3)

The above statements regarding the determination of the factor $\Delta P_{aв}/\Sigma P$ are also valid in the cases (1) and (2). During chemical transport, several heterogeneous equilibria can take place at the same time, therefore, when calculating the concentration gradient necessary for transport reactions, all these equilibria should be taken into account [7].

Publisher: **KOMAG Institute of Mining Technology, Poland**
© 2023 Author(s). This is an open access article licensed under the Creative Commons BY-NC 4.0 (https://creativecommons.org/licenses/by-nc/4.0/)

The main way to reverse the process is its conversion. In essence, the method is based on the reverse process of methane oxidation with steam, oxygen or carbon dioxide according to the following reaction:

$$CH_4 + H_2O \leftrightarrow CO + 3H_2$$
$$CH_4 + 0.5O_2 \leftrightarrow CO + 2H_2$$
$$CH_4 + CO_2 \leftrightarrow 2CO + 2H_2$$

It is possible to carry out "compatible" processes of steam-oxygen or steam-carbon conversion of natural gas (methane). Based on this, the reverse process can also be used for the processing of gaseous fuels produced during the direct LNG process.

The introduction of catalysts increases the rate of CH_4 conversion and lowers the temperature. The process takes place in the presence of a catalyst, which is formed during chemical transport at temperatures of 750÷780°C under conditions of reaching equilibrium. Despite the fact that the composition of methane in the mixture increases with increasing pressure, the conversion must take place under pressure in order to increase the reaction rate and reduce the volume of equipment and gas pipelines. In addition, all the processes of synthesis of organic products from CO and H_2 can take place at elevated pressures, therefore, when the conversion is carried out under pressure, the energy consumption for gas compression is reduced, which leads to energy savings.

It should be stated that the reversal is necessary, from the point of view of chemical thermodynamics, when the described conditions and processes are met.

4. Conclusions

According to the results of the evaluation of the received actual data of the modelling the technical conditions.

Implementation of the technology of reverse operations during the gasification of low-power coal seams at various stages of coal gasification at the LNG plant allowed for:

- reducing the time for ignition, burnout and formation of the reaction channel of the underground gas generator;
- creating the reaction, transition and recovery zones in a short time in an active-stable mode of activation of the process of thermochemical processes of gassing the coal seam;
- ensuring the appropriate length of the active reaction zones of the fire breakout in a stable temperature regime of gasification, taking into account the geo-mechanical parameters of the rock mass containing the gas generator, with increased convection heat exchange in the rock mass.
- maintaining the activity and stability of the gasification process in real conditions and given parameters during the gas generator attenuating mode, with the increase of the gassed space, changes in the integrity of the rocks of the roof and the floor of the coal seam, and the loss of leak tightness by the underground gas generator.

As it results from testing, in the cited research publications, the technological schemes, techniques and technology for reverse operations during borehole gasification of thin coal seams, characteristic for the coal deposits, have been presented.

References

[1] Bazaluk O., Lozynskyi V., Falshtynskyi V., Saik P., Dychkovskyi R., Cabana E.: Experimental Studies of the Effect of Design and Technological Solutions on the Intensification of an Underground Coal Gasification Process. Energies, 2021, 14(14), 4369. https://doi.org/10.3390/en14144369

[2] Dychkovskiy R., Bondarenko V.: Methods of Extraction of Thin and Rather Thin Coal Seams in the Works of the Scientists of the Underground Mining Faculty (National Mining University). International Mining Forum 2006, New Technological Solutions in Underground Mining, 2006, 21–25. https://doi.org/10.1201/noe0415401173.ch3

Publisher: **KOMAG Institute of Mining Technology, Poland**
© 2023 Author(s). This is an open access article licensed under the Creative Commons BY-NC 4.0 (https://creativecommons.org/licenses/by-nc/4.0/)

[3] Falshtynskyi V., Dychkovskyi R., Khomenko O., Kononenko M.: On the formation of a mine-based energy resource complex. E3S Web of Conferences, 2020, 201, 01020 https://doi.org/10.1051/e3sconf/202020101020

[4] Żogała A.: Critical Analysis of Underground Coal Gasification Models. Part I: Equilibrium Models – Literary Studies. Journal of Sustainable Mining, 2021, 13(1). https://doi.org/10.46873/2300-3960.1272

[5] Tabachenko M., Saik P., Lozynskyi V., Falshtynskyi V., Dychkovskyi R.: Features of setting up a complex, combined and zero-waste gasifier plant. Mining of Mineral Deposits, 2016, 10(3), 37–45. https://doi.org/10.15407/mining10.03.037

[6] Szewerda K., Krenicky T.: Use of the MBS method in mining industry R&D projects. Mining Machines, 2022, Vol. 40 Issue 2, pp. 110-120 https://doi.org/10.32056/KOMAG2022.2.6

[7] Pivnyak G., Falshtynskyi V., Dychkovskyi R., Saik P., Lozynskyi V., Cabana E., Koshka O.: Conditions of Suitability of Coal Seams for Underground Coal Gasification. Key Engineering Materials, 2020, 844, 38–48. https://doi.org/10.4028/www.scientific.net/kem.844.38

[8] Krichko A. A.: Theoretical Bases of Coal Gasification. Oils and Gases from Coal, 1980, 5, 89–124. https://doi.org/10.1016/b978-0-08-025678-8.50011-7

[9] Lentz N.: Gasification Systems. Mercury Control, 2014, 133–140. Portico. https://doi.org/10.1002/9783527658787.ch8

[10] Cabana E., Falshtynskyi V., Saik P., Lozynskyi V., Dychkovskyi R.: A concept to use energy of air flows of technogenic area of mining enterprises. E3S Web of Conferences, 2018, 60, 00004. https://doi.org/10.1051/e3sconf/20186000004

[11] Dvornikova E. V.: Environmental performance of underground coal gasification. Underground Coal Gasification and Combustion, 2018, 363–399. https://doi.org/10.1016/b978-0-08-100313-8.00031-1

[12] Falshtynskyi V., Dychkovskyi R., Lozynskyi V., Saik P.: Analytical, laboratory and bench test researches of underground coal gasification technology in National Mining University. New Developments in Mining Engineering, 2015, 97–106. https://doi.org/10.1201/b19901-19

[13] Blinderman M. S., Saulov D. N., Klimenko A. Y.: Forward and reverse combustion linking in underground coal gasification. Energy, 2008, 33(3), 446–454. https://doi.org/10.1016/j.energy.2007.10.004

[14] Liu H., Chen F., Wang Y., Liu G., Yao H., Liu S.: Experimental Study of Reverse Underground Coal Gasification. Energies, 2018, 11(11), 2949. https://doi.org/10.3390/en11112949

[15] Lozynskyi V., Dichkovskiy R., Saik P., Falshtynskyi V.: Coal Seam Gasification in Faulting Zones (Heat and Mass Balance Study). Solid State Phenomena, 2018, 277, 66–79. https://doi.org/10.4028/www.scientific.net/ssp.277.66

[16] Falshtynskyi V., Dychkovskyi R., Zasedatelev O.: Economic indicators of BUCG on an experimental station in the SC "Pavlogradvugillia" conditions. Technical and Geoinformational Systems in Mining, 2011, 201–206. https://doi.org/10.1201/b11586-33

[17] De Boer J. H., Van Arkel A. E.: Das Verhalten von Zirkoniumphosphat gegen Säuren und Basen. Zeitschrift Für Anorganische Und Allgemeine Chemie, 1925, 148(1), 84–86. Portico. https://doi.org/10.1002/zaac.19251480111

Publisher: **KOMAG Institute of Mining Technology, Poland**
© 2023 Author(s). This is an open access article licensed under the Creative Commons BY-NC 4.0 (https://creativecommons.org/licenses/by-nc/4.0/)

https://doi.org/10.32056/KOMAG2023.3.5

Optimization of support parameters for reusable mining excavations based on a neuro-heuristic prognostic model

Received: 18.09.2023

Accepted: 03.10.2023

Published online: 31.10.2023

Author's affiliations and addresses:

[1] Dnipro University of Technology, 19 Yavornytskoho Ave., UA-49005, Dnipro, Ukraine

[2] Mineral and Energy Economy Research Institute, Polish Academy of Sciences, J. Wybickiego, PL-31261, Krakow, Poland

[3] AGH University of Krakow, ave. Mickiewicza 30, PL-30059, Krakow, Poland

*** Correspondence:**

e-mail: Babets.d.v@nmu.one

tel.: +38 067 750 95 44

Dmytro BABETS [1], Olena SDVYZHKOVA [1], Artur DYCZKO [2], Łukasz GLIWIŃSKI [3]

Abstract:

This publication delves into geomechanical processes encountered during sequential longwall mining of coal seams, with a unique focus on reusing the conveyor track of the prior longwall as the ventilation pathway for the subsequent longwall. An in-depth geomechanical rationale is provided for the reuse of excavations within jointed rock formations. To ascertain the critical roles played by various support and protective elements at each distinct mining stage, a comprehensive analysis is performed using finite element techniques to delineate the three-dimensional stress-strain characteristics of the rock mass.
Employing an innovative methodology integrating multifactorial analysis, contemporary structural identification algorithms, and a neuro-heuristic approach for predictive mathematical modeling, an integral stability metric for reusable mining excavations is introduced. Specifically, this metric quantifies the relative preservation of the excavation's cross-sectional area following its connection to the second longwall. Furthermore, the study tackles the challenge of nonlinear optimization through the application of the generalized reduced gradient method (Frank-Wolfe), ultimately deriving the optimal combination of factors that maximizes the preservation of the cross-sectional area for these reusable excavations.

Keywords: longwall mining, coal seam, geomechanical processes, excavation reuse, jointed rocks, Finite Element Analysis, stress-strain analysis, support parameters, multifactorial analysis, nonlinear optimization

Publisher: **KOMAG Institute of Mining Technology, Poland**
© 2023 Author(s). This is an open access article licensed under the Creative Commons BY-NC 4.0 (https://creativecommons.org/licenses/by-nc/4.0/)

1. Introduction

Within the mining industry, a fundamental component of operational costs revolves around the establishment and upkeep of critical technological excavations (gateroads), including conveyor tracks (maingate), ventilation pathways (tailgate) etc. In recent years, Ukrainian mining operations have embarked on a path of modernization, driven by the imperative of achieving economically sustainable extraction levels. This transformation has entailed the overhaul of coal reserve preparation methodologies, with a significant shift towards adopting integrated longwall mining systems featuring backfilling techniques and the reutilization of essential technological excavations [1-3].

The proactive recreation of coal preparation infrastructure, both for active longwall mining operations and the provisioning of pre-prepared coal reserves, necessitates an unwavering commitment to reliability throughout all facets of mining technology. This commitment serves as the linchpin for ensuring seamless progress, curtailing downtime associated with equipment reconfiguration in novel mining zones, and substantially mitigating the risks linked to the maintenance of these vital excavations. The attainment of these objectives fundamentally hinges on the sustained operational integrity of reusable excavations [4-6].

Extensive research endeavors spanning multiple years, focused on evaluating the condition of preparatory excavations in mines within Western Donbas, have unveiled the intricate challenges inherent in supporting these excavations, particularly in areas influenced by neighboring longwall operations. These complexities are further compounded within the context of geologically weak and jointed rock formations. Numerous experimental investigations illustrate the increasing displacements within the gateroad when its cross-section intersects with the zone influenced by a longwall [7-10].

Based on accumulated experience in various conditions within Ukrainian mines and drawing from global expertise, different measures are employed to enhance the stability of excavations in areas influenced by coal extracting. However, integrating these individual measures into a comprehensive approach that is universally applicable to mines within a specific region necessitates a foundation rooted in the mechanics of coal-rock masses.

The parameters of support and protective systems are designed to be adjustable according to the magnitude and nature of the rock pressure manifestations, forecasted through a combination of accumulated experience, synthesis of empirical observations, and mathematical modeling of geomechanical processes.

Numerous studies have been dedicated to exploring geomechanical processes in the rock mass within the influence a longwall face [10-14]. However, insufficient attention has been devoted to the quantitative assessment of the impact of various stability assurance elements concerning the connection between technological excavations and longwall, particularly from the perspective of refining the technology of reinforcement and protection of technological excavations for the reuse purpose of their reuse [15].

2. Materials and Methods

2.1. Numerical three-dimensional modeling

We analyze the geomechanical processes within the rock mass at each stage, harnessing the advantages of numerical methods to determine the stress-strain state of the rock mass. In order to discern the role of various support and protection elements for excavations, we have considered a 3D model of the rock mass with a minimal number of layers: a coal seam with a thickness of 2.0 m and sandstone as a roof and floor of the gateroad.

The depth of the excavation is 400 meters, and the specific weight of the rock is assumed to be 25 kN/m³. Consequently, the vertical stresses in the intact rock mass amount to 10 MPa. The rock mass is considered as an elastic-plastic medium, with deformations following the Hoek-Brown strength theory. The modeling is carried out using RS3 software (Rocscience), which implements the finite element method in a three-dimensional setting. The model had dimensions of 200 × 50 × 50 m and was

Publisher: **KOMAG Institute of Mining Technology, Poland**
© 2023 Author(s). This is an open access article licensed under the Creative Commons BY-NC 4.0 (https://creativecommons.org/licenses/by-nc/4.0/)

divided into tetrahedron elements. The finite element analysis was conducted incrementally, ensuring that the deformations of rocks at a given stage were considered in the subsequent stage [16].

The computational framework for the three-dimensional modeling and the finite element mesh of the model are illustrated in Fig. 1.

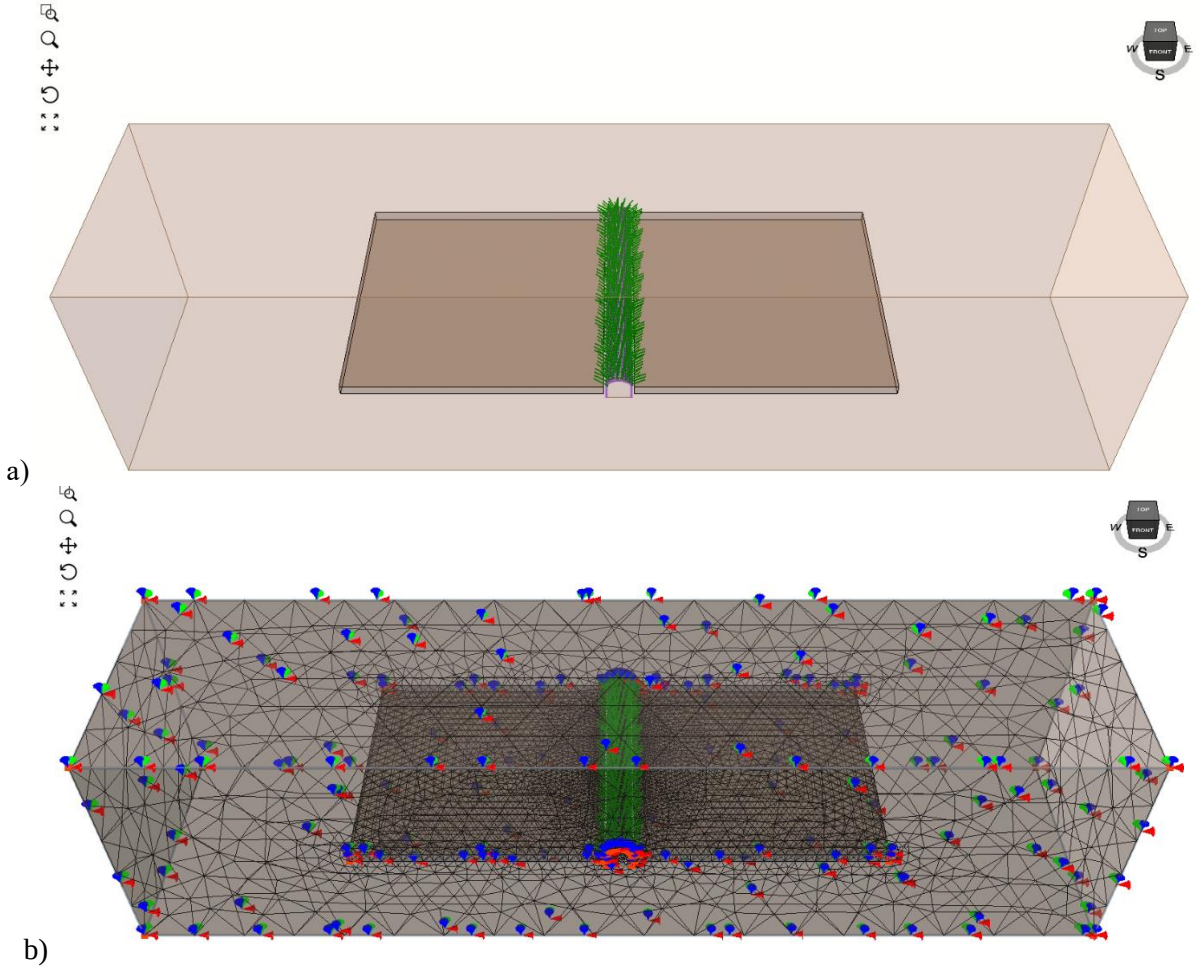

Fig. 1. Computational Scheme for Incremental Determination of Stress-Strain Components in the 'Longwall – gateroad - Longwall: a) Model Structure, b) Finite Element Mesh and restrains of the Model

In Fig. 2, the stages of three-dimensional modeling are depicted, simulating the creation of a gateroad and the gradual formation of the excavated space for two longwalls, as well as the development of rock displacements while considering various combinations of reinforcement and support.

At Stage 1, the gateroad in the intact mass is modeled, and support system is installed (Fig. 2a). At Stage 2, a void representing the first longwall is introduced by modifying boundary conditions (Fig. 2b). In Stage 3 (Fig. 2c), a void representing the second longwall is added. At this stage, the excavated space of the first longwall is replaced with material simulating the disintegrated rock mass after the overlying rock has collapsed. The characteristics of the stress-strain state of the rock mass are evaluated at each modeling step.

The initial data for the simulation are as follows: the mining depth; the gateroad dimensions; the coal seam thickness; the strength and deformation properties of the rock mass and coal seam; data on the rock jointness; parameters of the steel lining and the data on the rockbolt location. The parameters of a packwall made of wood or mineral binders to create a strong support pillar between the gateroad and mined-out space (a gob) should be also taken in consideration.

Publisher: **KOMAG Institute of Mining Technology, Poland**
© 2023 Author(s). This is an open access article licensed under the Creative Commons BY-NC 4.0 (https://creativecommons.org/licenses/by-nc/4.0/)

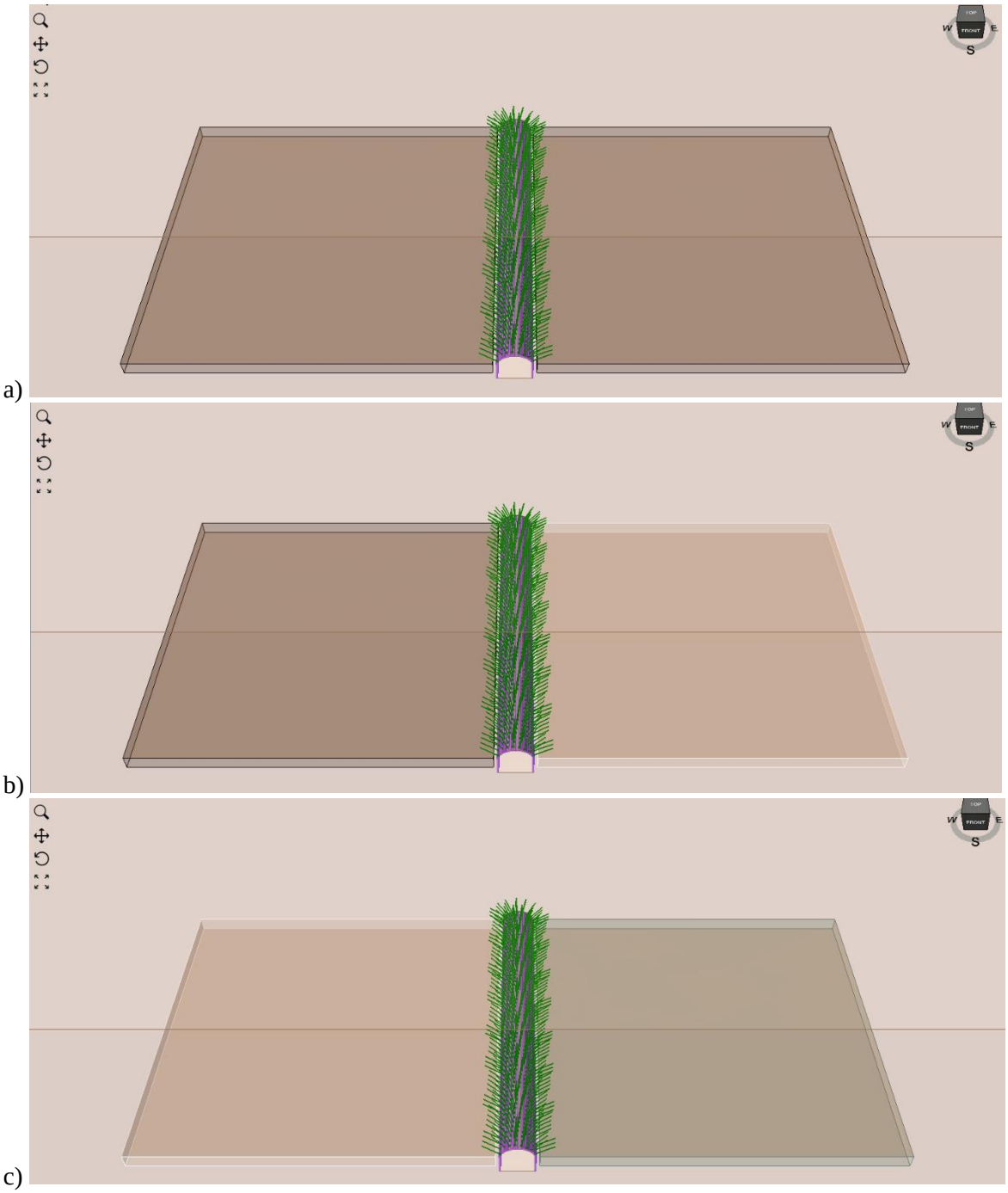

Fig. 2. The stages of mutual arrangement of longwalls and gateroad at different mining stages: a) Stage #1, b) Stage #2, c) Stage #3

The multi-variant three-dimensional modeling has enabled the identification of general trends in the development of rock displacements in the surrounding zone of connection between the excavation and the longwall. This forms the basis for constructing a predictive model.

2.2. The development of a multifactorial mathematical model for the stability of the reusable excavation

The execution of extensive numerical experiments allows for the generalization of deformation trends within the rock mass at various stages of longwall mining with the reuse of gateroads. Utilizing

Publisher: **KOMAG Institute of Mining Technology, Poland**
© 2023 Author(s). This is an open access article licensed under the Creative Commons BY-NC 4.0 (https://creativecommons.org/licenses/by-nc/4.0/)

the methodology developed in [17], which is based on modern structural identification algorithms and an inductive approach for creating predictive mathematical models, we introduce an integral indicator for ensuring the stability of the gateroad influenced by the excavated spaces of two longwalls.

As a suitable integral feature, it is prudent to select the relative value of the cross-sectional area of the gateroad that will be preserved after its connection with the second longwall.

In general, the problem of mathematical modeling can be formulated as follows: there are observational data or results from numerical experiments, and the objective is to construct a model to describe them. Subsequently, two possible scenarios may arise:

- When the model's structure is known (e.g., linear, quadratic, exponential, etc.), the task is solely to identify the model's parameters. This falls within the domain of parametric optimization.
- If the model's structure is unknown, the goal is to discover the optimal model and identify its parameters, which are optimal according to a predictive criterion. This constitutes the problem of structural optimization (identification).

In this research, we focus on generating a multifactorial mathematical model for the stability analysis of preparatory operations, using a structural identification approach.

Group Method of Data Handling (GMDH) is a machine learning and data analysis technique used for regression and classification tasks. GMDH is an algorithmic approach that belongs to the family of machine learning methods known as self-organizing data analysis techniques [18].

The key idea behind GMDH is to develop a model that can capture complex relationships between input variables (features) and output variables (target) by creating a series of polynomial equations. These equations are generated through a process of group modeling and optimization. GMDH builds a series of models, each more complex than the previous one, and selects the best model based on certain criteria, often aiming for the best trade-off between model accuracy and complexity.

The complexity of the model structure is assessed based on the number of polynomial terms. The iterative search procedure involves calculating the criterion while gradually increasing the complexity of the model structure. When selecting the model structure, we are guided by two principles: to strive for the model to be as simple as possible (the principle of parsimony) and to improve the model by assessing its adequacy and predictive properties (the principle of adequacy).

A distinctive GMDH feature is the organization of the search for the optimal model structure using both internal and external selection criteria. A criterion is termed internal if it is calculated over the entire data sample. An external criterion is calculated using new information that was not used to estimate the model coefficients [19]. Therefore, to ensure the model's quality predictive properties, i.e., its stability concerning new data, it is necessary to divide the entire dataset into two parts. The first dataset is used for model construction and is referred to as the training data. The second dataset serves as new data and is used to assess the quality of the constructed model. This dataset is known as the validation data.

The methodology applied in these studies is as follows:

- Determine a class of models with increasing complexity.
- Divide the data (Experimental Data = Training Data + Validation Data).
- For a given level of complexity, estimate the model parameters using the first dataset (training data) and apply an internal criterion.
- Validate the model using the second dataset with the application of an external criterion.
- If the external criterion reaches a minimum, the best model has been found; otherwise, it is necessary to increase the model's complexity and return to step 3.

In terms of their structure, GMDH algorithms are closely related to self-learning algorithms for multilayer pattern recognition systems or neural networks [20]. The significant difference lies in the fact that polynomial GMDH algorithms operate with continuous variables. Only continuous variables allow for finding the minimum of an external criterion, which determines the optimal structure of the mathematical model.

Publisher: **KOMAG Institute of Mining Technology, Poland**
© 2023 Author(s). This is an open access article licensed under the Creative Commons BY-NC 4.0 (https://creativecommons.org/licenses/by-nc/4.0/)

2.3. The formulation of a problem for conditional optimization

To determine the most rational combination of factors in order to preserve the maximum cross-section of reusable gateroad, we will solve a problem of constrained optimization of a multivariable function obtained using the GMDH algorithm.

The method of reduced gradient can be considered as a nonlinear extension of the simplex method, which selects a basis, determines the search direction, and performs linear search in any large iterative system of nonlinear equations at each step.

The Generalized Reduced Gradient Method (Frank-Wolfe) uses second-order derivative approximations to accelerate the process and verify whether the optimal solution has been found. It is an advancement of the reduced gradient method and can be applied to solve problems with nonlinear constraints [21, 22].

Let's consider the algorithm of the Generalized Reduced Gradient Method for solving the problem:

$$max\, F = f(x_1, x_2, \dots, x_n) \tag{1}$$

under the following restrictions:

$$\sum_{j=1}^{n} a_{ij} x_j \le b_i\,,\ \ (i = \overline{1,m}) \tag{2}$$

$$x_j \ge 0,\ \ (j = \overline{1,n}) \tag{3}$$

A characteristic feature of problems solvable using this method is that their system of constraints should only contain linear inequalities. This feature forms the basis for replacing the nonlinear objective function with a linear one in the vicinity of the examined point. As a result, solving the original problem is reduced to sequentially solving linear programming problems [23, 24].

Algorithm of the method is as follows. Determine a point belonging to the feasible region. Let this point be denoted as $X^{(k)}$. Then, compute the gradient of the function at this point

$$\nabla f(X^{(k)}) = \left[\frac{\partial f(X^{(k)})}{\partial x_1}, \frac{\partial f(X^{(k)})}{\partial x_2}, \dots, \frac{\partial f(X^{(k)})}{\partial x_n}\right]$$

and form a linear function:

$$F = \frac{\partial f(X^{(k)})}{\partial x_1} x_1 + \frac{\partial f(X^{(k)})}{\partial x_2} x_2 + \dots + \frac{\partial f(X^{(k)})}{\partial x_n} x_n \tag{4}$$

We proceed to a new problem, which involves maximizing the function (4) subject to constraints (2) and (3). Let the solution to this problem be determined by the point $Z^{(k)}$. Then, the coordinates of point $X^{(k+1)}$ are taken as the new feasible solution for the original problem (1) - (3).

$$X^{(k+1)} = X^{(k)} + \lambda_k (Z^{(k)} - X^{(k)}), \tag{5}$$

where λ_k is a certain number called the computation step, and its value should be between zero and one, meaning $0 \le \lambda_k \le 1$. This step λ_k is usually chosen arbitrarily or determined in such a way that the value of the function at point $X^{(k+1)}(f(X^{(k+1)})$, which depends on λ_k, is maximized. To do this, it is necessary to find the solution to the equation:

$$\partial f(X^{(k+1)})/\partial \lambda_k = 0$$

and select its maximum root. If the value obtained in this way turns out to be greater than one, then set $\lambda_k = 1$.

After determining λ_k, you find the coordinates of the point $X^{(k+1)}$, calculate the value of the objective function at that point, and, using the inequality:

$$\left| f(X^{(k+1)} - f(X^{(k)}) \right| < \varepsilon \tag{6}$$

Publisher: **KOMAG Institute of Mining Technology, Poland**
© 2023 Author(s). This is an open access article licensed under the Creative Commons BY-NC 4.0 (https://creativecommons.org/licenses/by-nc/4.0/)

(where ε is a sufficiently small number), it is determined whether it is necessary to transition to a new point $X^{(k+2)}$. If such a necessity exists (the inequality is not satisfied), then the gradient of the objective function is calculated at the point $X^{(k+1)}$.

Then we proceed to the corresponding linear programming problem, find its solution, determine the coordinates of point $X^{(k+2)}$, and investigate the necessity of further computations. It should be noted that after performing a finite number of such steps, a solution to the original nonlinear programming problem (1)-(3) is obtained with the required accuracy.

This algorithm has been applied to find the optimal support parameters for the predictive function of preserving the reusable excavation cross-section.

3. Results

3.1. Results of numerical modeling of the stress-strain state of the rock mass

A multifactor computational experiment was conducted. Under other equal conditions, the following parameters were varied: "relative width of the protective element" (w/m) within a range from 0.6 to 0.8; the stiffness of the protective element (k_n) with a range of variation from 0 to 10^4 MPa/m.

The creation of a stable rock lining is not possible without the implementation of a rational roof bolting scheme [25]. To quantitatively consider the parameters of roof bolting, we introduce the generalized factor "relative number of bolts per cross-sectional area of the excavation" (Na), which varies from 0 (without roof bolting) to 0.6 (11 bolts, relative to a cross-sectional area of 17.7 m^2). Another factor characterizing the support system is "spacing of the installation of the metal arch support" (q) with a range of variation from 0.5 to 1 m.

The fifth integral factor introduced into the analysis is the parameter of mining conditions according to Yu. Zaslavsky [26], which is the ratio of the initial stress field γH to the uniaxial compression strength of rocks. This factor varies within the range of 0.3 - 0.7 in terms of Western Donbas coal mines. For a full factorial analysis, it is necessary to perform 3^5 experiments, i.e., the calculation of 243 finite element models was conducted.

The result of the modeling is the maximum displacements in the roof and floor of the excavation, as well as the total preservation of the gateroad cross-section.

For each combination of the varied factors provided by the computational experiment plan, modeling was carried out by organizing three stages, each of which corresponds to a specific stage of the mutual arrangement of the excavation and two longwalls.

The displacement of the excavation contour for one of the 243 numerical models is shown in Fig. 3.

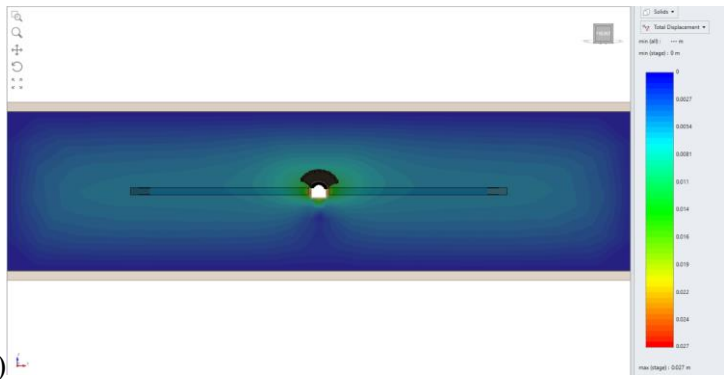

a)

Publisher: **KOMAG Institute of Mining Technology, Poland**
© 2023 Author(s). This is an open access article licensed under the Creative Commons BY-NC 4.0 (https://creativecommons.org/licenses/by-nc/4.0/)

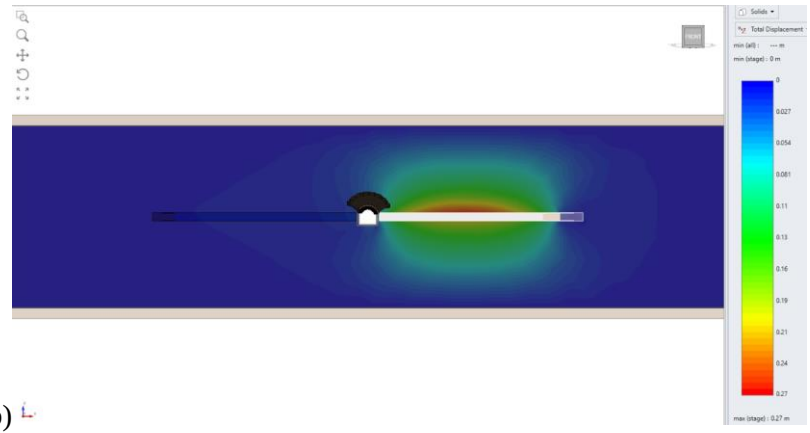

b)

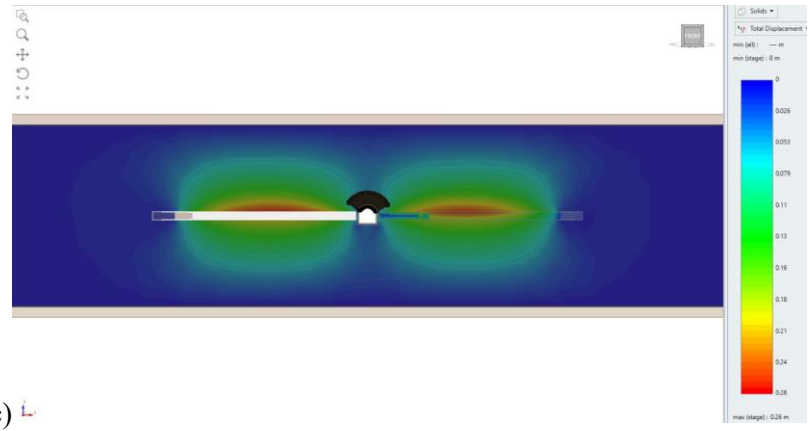

c)

Fig. 3. Development of displacements during longwall mining: a) excavation of a gateroad in the intact mass; b) formation of the excavated space of the first longwall; c) formation of the excavated space of the second longwall and filling the excavated space of the first longwall with disintegrated material

The purpose of the computational experiment is to establish the dependence of the initial data - maximum displacements in the roof and floor of the excavation and total preservation of the cross-section - on the varied factors.

3.2. Creation of a predictive model and optimization of support parameters.

The execution of extensive numerical experiments allowed us to generalize the trends in the development of rock mass displacements at various stages of longwall mining with the gateroad reuse.

The fragments of initial data for the GMDH analysis and the corresponding values of the percentage of the gateroad cross-section that will be preserved (based on multi-variant modeling results) after merging with the second longwall are presented in Table 1.

Table 1. Data for GMDH analysis of the gateroad stability

	γH/Rc	K_n, MPa/m	N_a	w/m	q, m	preserved cross-section (S), %
№	0.3-0.7	0-10000	0-0.6	0.6-0.8	0.5-1	
1	0.3	0	0.00	0.6	1	12
2	0.7	0	0.00	0.6	1	10
3	0.3	10000	0.00	0.6	1	17
4	0.3	0	0.51	0.6	1	14

Publisher: **KOMAG Institute of Mining Technology, Poland**
© 2023 Author(s). This is an open access article licensed under the Creative Commons BY-NC 4.0 (https://creativecommons.org/licenses/by-nc/4.0/)

5	0.3	0	0.00	0.8	1	15
6	0.3	0	0.00	0.6	0.5	16
7	0.3	10000	0.51	0.6	1	27
8	0.3	10000	0.00	0.8	0.5	25
9	0.3	10000	0.51	0.8	0.5	70
10	0.7	10000	0.51	0.8	0.5	60
11	0.3	5000	0.51	0.8	0.5	68
12	0.3	10000	0.28	0.8	0.5	55
13	0.5	5000	0.28	0.7	0.75	50
14	0.3	3000	0.28	0.8	0.5	62
15	0.7	5000	0.17	0.6	0.5	50
16	0.5	5000	0.40	0.8	1	48
17	0.7	8000	0.17	0.7	0.5	52
18	0.3	10000	0.40	0.6	0.75	53
19	0.6	10000	0.40	0.6	0.75	43
20	0.3	5000	0.17	0.6	0.5	41
21	0.4	5000	0.28	0.7	0.75	50
22	0.6	2500	0.17	0.7	1	29
23	0.4	8000	0.45	0.8	0.6	65
24	0.7	10000	0.51	0.7	0.5	52
25	0.8	10000	0.51	0.8	0.5	55
…	…	…	…	…	…	…

The data from Table 1 were processed using combinatorial and iterative algorithms of Group Method of Data Handling. The dependency generated by the iterative algorithm was selected as the most adequate predictive model based on the minimum external criterion.

$$S = \frac{w}{m} \cdot \left(218N_a - 14\frac{\gamma H}{R_c}\right) + 0.017k_n^{2/3} - 186N_a^2 - 9{,}9q^2 + 25 \tag{7}$$

The coefficient of determination is 0.94 for the training subset and 0.92 for the validation subset. Theaverage value for the entire investigated data set is R^2=0.93.

The graphical adequacy of the predictive model (7) is visualized in Figure 4. The input values for the GMDH analysis are shown in gray, the values of the function (7) obtained for the training subset of data are shown in blue, and the results of the forecast and the confidence interval are shown in red.

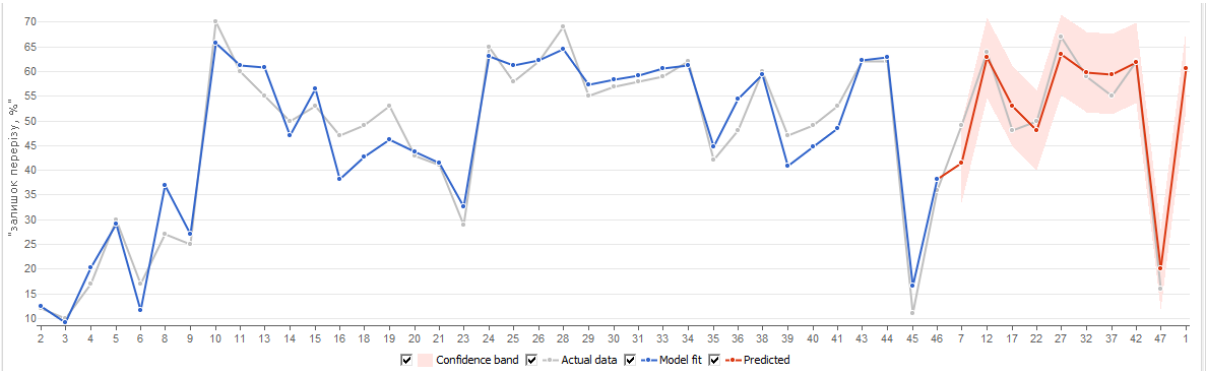

Fig. 4. Visualization of the predictive model for preserving the cross-sectional area of the reusable excavation

Publisher: **KOMAG Institute of Mining Technology, Poland**
© 2023 Author(s). This is an open access article licensed under the Creative Commons BY-NC 4.0 (https://creativecommons.org/licenses/by-nc/4.0/)

The influence of each factor, weighted by coefficients, on the resulting indicator is as follows: “relative number of bolts per cross-sectional area of the excavation” (N_a) - 32%, “relative width of the protective element” (w/m) - 28%, 'spacing of the installation of the metal arch support' (q) - 18%, development parameter ($\gamma H/\sigma$) - 13%, and the stiffness of the protective element (k_n) - 9%.

To determine the most rational combination of factors for the purpose of preserving the maximum cross-sectional area of the reusable excavation, we will solve a multi-variable conditional optimization problem.

Using the generalized reduced gradient method, we have solved the problem (1)-(3) for the predictive function (7). As a result of the optimization, it was determined that the maximum of the function (7) under the specified constraints of input variables is

$$S_{max}(N_a, w/m, q, kn, \gamma H/Rc)=67.9\%$$

So, with the best combination of input variables, it is forecasted that up to 68% of the cross-sectional area of the reusable excavation, influenced by two longwalls will be preserved. The maximum is achieved with the following variable values: N_a = 0.47; w/m = 0.8; q = 0.5; k_n = 10 000 MPa/m, $\gamma H/\sigma$ = 0.3. It should be noted that these values of the factors (Na, w/m, q, k_n) are optimal for all values of the parameter of mining condition within its range of variation (from 0.3 to 0.7).

Therefore, it should be noted that the prospects of reusing excavations are largely determined by a complex of geomechanical and technological parameters during the final sections of the longwall mining, ensuring the stability of the gateroad. Further maintenance does not pose significant difficulties, taking into account the implementation of appropriate repair and restoration measures. However, the scope of these measures is significantly reduced with adequate forecasting of rock pressure and the design of an appropriate support and protection system for the excavation.

4. Conclusions

1. Multivariate modeling of the "longwall - reusable gateroad - longwall" system has demonstrated that sequential installing various support elements into the model, such as metal arch supports, steel-polymer bolts, and cable bolts, the role of each of them in ensuring excavation stability has been highlighted and has served as the basis for generalized analysis using the Group Method of Data Handling (GMDH). Thus, the role, feasibility, and sequence of measures to ensure the stability of gateroads, sufficient for their reuse, have been substantiated.
2. Using the Group Method of Data Handling (GMDH) based on modern structural identification algorithms and an inductive approach to create predictive mathematical models, a relationship has been obtained for the residual cross-sectional area of the excavation, which serves as an integral indicator of the stability of preparatory excavations influenced by two longwalls. This relationship is dependent on mining-geological and mining-technical parameters, the significance of which has been justified in the research. These parameters include the relative width of the protective element (w/m), the contact stiffness coefficient in the protective element (k_n), the number of roof bolts per cross-sectional area of the excavation (N_a), the spacing of the installation of the metal arch support (q), and the parameter of development conditions ($\gamma H/\sigma$). It has been determined that the influence of each factor on the resulting indicator is as follows: N_a - 32%, w/m - 28%, q - 18%, k_n - 9%, and $\gamma H/\sigma$ - 13%.
3. Using the Generalized Reduced Gradient Method (Frank-Wolfe), the problem of nonlinear optimization for the obtained multifactor function - the residual cross-sectional area of the excavation (7) - has been solved, and optimal parameters have been determined. These parameters maximize the function, ensuring the preservation of the maximum cross-sectional area of the reusable excavation influenced by two longwalls.

Publisher: **KOMAG Institute of Mining Technology, Poland**
© 2023 Author(s). This is an open access article licensed under the Creative Commons BY-NC 4.0 (https://creativecommons.org/licenses/by-nc/4.0/)

References

[1] Haidai O., Ruskykh V., Ulanova N., Prykhodko V., Cabana E. C., Dychkovskyi R., Howaniec N., Smolinski A.: Mine field preparation and coal mining in western Donbas: Energy security of Ukraine – a case study. Energies, 2022, 15(13), 4653. https://doi.org/10.3390/en15134653

[2] Kovalevska I., Samusia V., Kolosov D., Snihur V., Pysmenkova T.: Stability of the overworked slightly metamorphosed massif around mine working. Mining of Mineral Deposits, 2020, 14(2), 43–52. https://doi.org/10.33271/mining14.02.043

[3] Vlasov S. F., Moldavanov Ye. V.: Effect of geological and technological parameters on the convergence in a Stope. Naukovyi Visnyk Natsionalnoho Hirnychoho Universytetu, 2021, (6), 16–22. https://doi.org/10.33271/nvngu/2021-6/016

[4] Liu H., Jiang Z., Chen W., Chen F., Ma F., Li D., Liu Z., Gao H.: A simulation experimental study on the advance support mechanism of a roadway used with the longwall coal mining method. Energies, 2022, 15(4), 1366. https://doi.org/10.3390/en15041366

[5] Yang X., Huang R., Yang G., Wang Y., Cao J., Liu J., He M.: Validation study of no-pillar mining method without advance tunneling: A case study of a mine in China. Energy Science & Engineering, 2021, 9(10), 1761–1772. https://doi.org/10.1002/ese3.949

[6] Gao Y., Gai Q., Zhang K., Fu Q., Zhang X.: Strata behaviour and stability control of the automatic roadway formation by roof cutting below a fault influenced Longwall Goaf. Scientific Reports, 2022, 12(1). https://doi.org/10.1038/s41598-022-20810-7

[7] Jangara H., Ozturk C. A.: Longwall top coal caving design for thick coal seam in very poor strength surrounding strata. International Journal of Coal Science & Technology, 2021, 8(4), 641–658. https://doi.org/10.1007/s40789-020-00397-y

[8] Wang J., Yang S., Wei W., Zhang J., Song Z.: Drawing mechanisms for top coal in longwall top coal caving (LTCC): A review of two decades of literature. International Journal of Coal Science & Technology, 2021, 8(6), 1171–1196. https://doi.org/10.1007/s40789-021-00453-1

[9] Petlovanyi M. V., Lozynskyi V. H., Saik P. B., Sai K. S.: Modern experience of low-coal seams underground mining in Ukraine. International Journal of Mining Science and Technology, 2018, 28(6), 917–923. https://doi.org/10.1016/j.ijmst.2018.05.014

[10] Li Y., Zhu E., Zhang K., Li M., Wang J., Li C.: Longwall mining under gateroads and gobs of abandoned small mine. International Journal of Mining Science and Technology, 2017, 27(1), 145–152. https://doi.org/10.1016/j.ijmst.2016.11.004

[11] Babets D. V., Sdvyzhkova O. O., Sosna D. O.: Numerical simulation of the joint conditions effect on the rock mass strength. Journal of Kryvyi Rih National University, 2018, (47), 169–175. https://doi.org/10.31721/2306-5451-2018-1-47-169-175

[12] Shi X., Zhang J.: Characteristics of overburden failure and fracture evolution in shallow buried working face with large mining height. Sustainability, 2021, 13(24), 13775. https://doi.org/10.3390/su132413775

[13] Singh G. S. P.: Conventional approaches for assessment of caving behavior and support requirement with regard to strata control experiences in longwall workings. Journal of Rock Mechanics and Geotechnical Engineering, 2015, 7(3), 291–297. https://doi.org/10.1016/j.jrmge.2014.08.002

[14] Prykhodchenko V. F., Shashenko O. M., Sdvyzhkova O. O., Prykhodchenko O. V., Pilyugin V. I.: Predictability of a small-amplitude disturbance of coal seams in western Donbas. Naukovyi Visnyk Natsionalnoho Hirnychoho Universytetu, 2020, (4), 024–029. https://doi.org/10.33271/nvngu/2020-4/024

[15] Babets D., Sdvyzhkova O., Hapieiev S., Shashenko O., Prykhodchenko V.: Multifactorial analysis of a gateroad stability at goaf interface during longwall coal mining – a case study. Mining of Mineral Deposits, 2023, 17(2), 9–19. https://doi.org/10.33271/mining17.02.009

[16] Babets D, Sdvyzhkova O., Shashenko O., Kravchenko K., Cabana E. C.: Implementation of probabilistic approach to rock mass strength estimation while excavating through fault zones. Mining of Mineral Deposits, 2019, 13(4), 72–83. https://doi.org/10.33271/mining13.04.072

Publisher: **KOMAG Institute of Mining Technology, Poland**
© 2023 Author(s). This is an open access article licensed under the Creative Commons BY-NC 4.0 (https://creativecommons.org/licenses/by-nc/4.0/)

[17] Shashenko O.M., Sdvyzhkova O.O., Babets D.V.: Method of argument group account in geomechanical calculations. 12th International Symposium on Environmental Issues and Waste Management in Energy and Mineral Production SWEMP 2010, 2010, 488–493

[18] Babets D., Solodyankin O., Yankin O.: Mathematical modeling of the external factors influence on the margin of strength while shaft sinking. Transactions of Kremenchuk Mykhailo Ostrohradskyi National University, 2018, 65–72. https://doi.org/10.30929/1995-0519.2018.1.65-72

[19] Madala H. R., Ivakhnenko A. G.: Inductive learning algorithms for Complex Systems modeling. CRC Press, 2018

[20] Elbaz K., Shen S.-L., Zhou A., Yin Z.-Y., Lyu H.-M.: Prediction of disc cutter life during shield tunneling with AI via the incorporation of a genetic algorithm into a GMDH-type neural network. Engineering, 2021, 7(2), 238–251. https://doi.org/10.1016/j.eng.2020.02.016

[21] Facó J. L. D.: A generalized reduced gradient algorithm for solving large-scale discrete-time Nonlinear Optimal Control Problems. IFAC Proceedings Volumes, 1989, 22(2), 45–50. https://doi.org/10.1016/b978-0-08-037869-5.50011-x

[22] Dychkovskyi R., Falshtynskyi V., Ruskykh V., Cabana E., Kosobokov O.: A modern vision of simulation modelling in mining and near mining activity. E3S Web of Conferences, 2018, 60, 00014. https://doi.org/10.1051/e3sconf/20186000014

[23] El Mouatasim A.: Two-phase generalized reduced gradient method for constrained global optimization. Journal of Applied Mathematics, 2010, 1–19. https://doi.org/10.1155/2010/976529

[24] Dyczko A.: Real-time forecasting of key coking coal quality parameters using neural networks and artificial intelligence. Rudarsko-Geološko-Naftni Zbornik, 2023, 38(3), 105–117. https://doi.org/10.17794/rgn.2023.3

[25] Tereshchuk R. M., Khoziaikina N. V., Babets D. V.: Substantiation of rational roof-bolting parameters. Scientific Bulletin of National Mining University, 2018, 1, 19–26. https://doi.org/10.29202/nvngu/2018-1/18

[26] Babets D. V.: Development of rock mass stability classification depending on natural disturbances. Transactions of Kremenchuk Mykhailo Ostrohradskyi National University, 2016, 2(97), 44-51

Publisher: **KOMAG Institute of Mining Technology, Poland**
© 2023 Author(s). This is an open access article licensed under the Creative Commons BY-NC 4.0 (https://creativecommons.org/licenses/by-nc/4.0/)

https://doi.org/10.32056/KOMAG2023.3.6

Pressure analysis and control in an industrial gas heating furnace as a way to reduce CO_2 emission

Received: 16.10.2023

Accepted: 26.10.2023

Published online: 31.10.2023

Author's affiliation and address:

[1] Silesian University of Technology, Faculty of Materials Engineering, Krasińskiego 8, 40-019 Katowice

*** Correspondence:**

e-mail: mariusz.wnek@polsl.pl

Mariusz WNĘK [1*]

Abstract:

Emission of carbon dioxide, which may affect the greenhouse effect leading to global warming is a critical aspect of the industrial use of thermal devices. The article presents the results of testing the combustion processes in the operating conditions in an industrial heating device fired by gas burners. technical, energy and operational parameters of the selected chamber for thermal process of the selected fuel input were characterized and analysed. A solution related to pressure control in the combustion chamber, which should be used to reduce the level of CO_2 emissions, which will enable a positive environmental impact is presented. Pro-ecological character of the presented solution is a very important practical effect. Especially nowadays, when there is a strong need to reduce the negative impact of production processes on environment, and all solutions leading to a reduction in CO_2 emission should also be perceived as very important for business.

Keywords: burning of fuels, combustion chamber, gas burners, gas fuel savings, reduced emission of CO_2

Publisher: **KOMAG Institute of Mining Technology, Poland**
© 2023 Author(s). This is an open access article licensed under the Creative Commons BY-NC 4.0 (https://creativecommons.org/licenses/by-nc/4.0/)

1. Introduction

The economic aspect is the basis for eliminating the energy losses in the steel industry energy systems - which are the main industrial problem. Another very important issue that has emerged in recent years is the environmental protection. However, this aspect is not a natural need of steel industry energy enterprises but rather results from the requirements imposed by standards, laws or obligations. Economic factors are often an incentive for pro-ecological activities - discounts, access to cheap investment loans or even the possibility of additional funds [1]. Therefore, in the analysis of the presented problem, this issue is assessed in terms of below two aspects.

The following installations can be distinguished in the types of facilities selected for analysis:

a) fuel,

b) combustion air,

c) exhaust gas discharge,

and the systems:

a) temperature control of the technological process,

b) control of the amount of excess combustion air,

c) control of pressure in the combustion chamber,

d) control of oxygen concertation in exhaust gases.

Any actions that reduce consumption of gas fuel result in lower costs as well as reduced exhaust gases emission including: CO_2, which is an additional environmental aspect. Reducing the carbon dioxide emission may also have an economic aspect related to CER [2].

CER (Certified Emission Reduction) is one of the emissions trading units used under the Kyoto Protocol, which is part of the United Nations Framework Convention on Climate Change (UNFCCC). CER is emitted as a result of projects to reduce greenhouse gas emission in developing countries that are parties to the Kyoto Protocol. These projects must meet specific criteria and be approved by the Clean Development Mechanism (CDM), which is part of the Kyoto Protocol. The main goal of CDM projects is to reduce greenhouse gas emission, especially carbon dioxide (CO_2), through the use of more sustainable technologies or operating practices.

Once the project has been approved and the CER has been obtained, these credits can be sold, for example, on the international emissions market or on domestic markets, where they are used to meet countries' or companies' greenhouse gas emission reduction commitments. CERs play an important role in international efforts to reduce greenhouse gas emissions and fight climate change [2-5].

Savings from reducing the consumption of gas fuel and participation in the trade in CO_2 emission certificates may provide a given company with additional and significant funds that can be invested in any way, e.g. in the development of the company, modernization or improvement of employees qualifications.

2. Materials and Methods (Assumptions)

Analysis of main energy problems of installations and systems used in metallurgical industry and utility energy systems was carried out on the basis of continuous and chamber metallurgical heating furnaces [6, 7]. A proposal to solve the discussed problem based on operational tests is presented. The paper discusses a significant economic problem, the solution of which may bring significant economic savings as well as a positive impact on the environment.

Proper selection of the control component, i.e. valves (for gaseous fuel and air) with appropriate flow characteristics and an actuator with appropriate setting accuracy and variable rotational speed [8] is an important element in the characteristics control. The characteristics of the setting components should be close to linear, what would significantly facilitate control [9].

Publisher: **KOMAG Institute of Mining Technology, Poland**
© 2023 Author(s). This is an open access article licensed under the Creative Commons BY-NC 4.0 (https://creativecommons.org/licenses/by-nc/4.0/)

Linearization of flow refers to the process of transforming nonlinear flow relationships of liquids or gases into approximate linear relationships to facilitate the analysis, design, and control of flow systems. This is particularly useful in engineering such as chemical engineering, fluid mechanics, and automation.

Flow linearization involves approximating nonlinear equations describing the flow using the linear differential equations or difference equations around a certain operating point or equilibrium point. The operating point is the state in which the system is stable and in equilibrium.

The linear model obtained by linearization can be used to analyse system stability, design controllers, and predict system behaviour in response to variable operating conditions or input changes.

3. Pressure in an industrial heating furnace

3.1. Pressure control in a combustion chamber

Temperature – resulting from the requirements of the technological process is the most important parameter controlled in industrial heating furnaces fired with gas fuel. The gas fuel stream depends on the set furnace temperature, while air and exhaust gases mass flow follow the fuel stream and should be proportional to it [9, 10, 11]. However, the exhaust gas flow is very difficult to measure, therefore it cannot be a controlled parameter. Measurable and therefore the controlled parameter can be the exhaust gas pressure in the furnace, the value of which is usually in the range $p_E \in$ [-30 ÷ +30] Pa and is a function of the exhaust gas stream discharged into the chimney, so it depends on the degree of opening of the chimney gate valve or damper and on the exhaust gas temperature.

Depending on the ratio $\dot{m}_E$ (discharged by the exhaust system) to $\dot{m}_{EB}$ (exhaust gases produced in the burners), a negative or overpressure is generated in the furnace. Both cases lead to a drop in the furnace temperature and a reduction in its thermal efficiency, although the mechanism of these unfavourable phenomena is different in both cases. An additional problem that occurs with negative pressure is the increase in the share of oxygen in the O_{2E} exhaust gases and thus the formation of an oxidizing atmosphere in a furnace.

Therefore, the exhaust gas pressure in the heating furnace chamber is, or rather should be, one of the main controlled parameters. The correct distribution of static pressure is an important factor for proper operation of the furnace, but it is not uniform in the working space (Fig. 1).

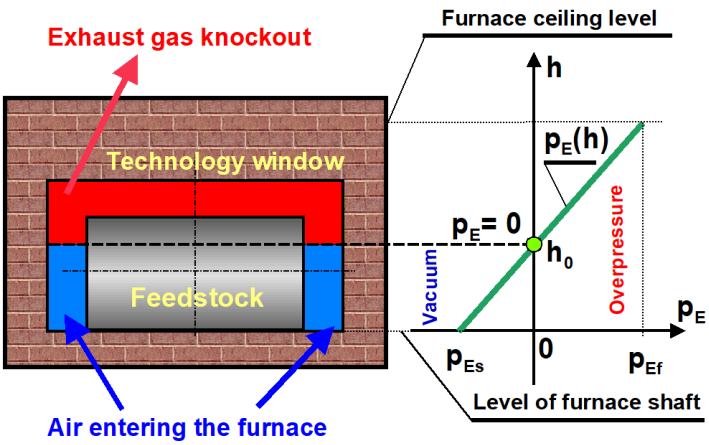

Fig. 1. View of the technological window and distribution of manometric exhaust gas pressure relative to the height of the furnace

Publisher: **KOMAG Institute of Mining Technology, Poland**
© 2023 Author(s). This is an open access article licensed under the Creative Commons BY-NC 4.0 (https://creativecommons.org/licenses/by-nc/4.0/)

Considering additionally state-of-the-art heating solutions, such as recuperative or regenerative burners, the distribution of manometric pressure in the furnace can be described by the following relationship:

$$p_E(h) = p_{EB}(h_B) + g(\rho_A - \rho_E)h \tag{1}$$

where:

ρ_A – atmospheric air density, kg/m^3;

ρ_E – density of exhaust gases in a furnace, kg/m^3;

g – acceleration due to gravity, m/s^2;

h_B – position of the burner in relation to the furnace shaft, m.

Equation (1) shows that the distribution of pressure in the furnace is influenced by the following:

- position of burners with regenerators in relation to the furnace shaft – h_B,
- pressure p_{EB} generated at the inlet by the burner sucking exhaust gases (for recuperative or regenerative burners),
- surface area of the slot in the feeding window *A(h)*.

Therefore, when the furnace is operating, it is very important to maintain the proper distribution of exhaust gas pressure in the combustion chamber, which is a significant controlling problem. The basis of this problem is that most industrial heating furnaces do not have automatic control of exhaust gas pressure or existing solutions do not meet their destination.

The solution to this problem is related to:

- selection of a sensor to measure small values of exhaust gas manometric pressure,
- selection or design of an adjusting component with appropriate flow characteristics to control the exhaust gas stream [11, 12, 13],
- determining the optimal exhaust gas pressure p_{Eopt} at which the sum of energy losses caused by false air entering the furnace (2) and exhaust gases escaping into the surroundings (3) through the gaps in the technological windows is minimal,
- selection of a PLC controller or regulator and its settings.

$$d\dot{m}_{Ao} = \alpha \cdot dA(h)\sqrt{2 \cdot p_E(h) \cdot \rho_A} \tag{2}$$

$$d\dot{m}_{Eo} = \alpha \cdot dA(h)\sqrt{2 \cdot p_E(h) \cdot \rho_E} \tag{3}$$

where:

α – flow number 0.7 ÷ 0.8;

A(h) – a slot surface area, m^2;

$p_E(h)$ – manometric pressure in the furnace, Pa;

ρ_A – air density, kg/m^3;

ρ_E - density of exhaust gases in the furnace, kg/m^3.

Publisher: **KOMAG Institute of Mining Technology, Poland**
© 2023 Author(s). This is an open access article licensed under the Creative Commons BY-NC 4.0 (https://creativecommons.org/licenses/by-nc/4.0/)

Moreover, to properly control the exhaust gas pressure of the heating furnace, it is necessary to know the temperature and pressure control characteristics (Fig. 2) and the energy characteristics (Fig. 3).

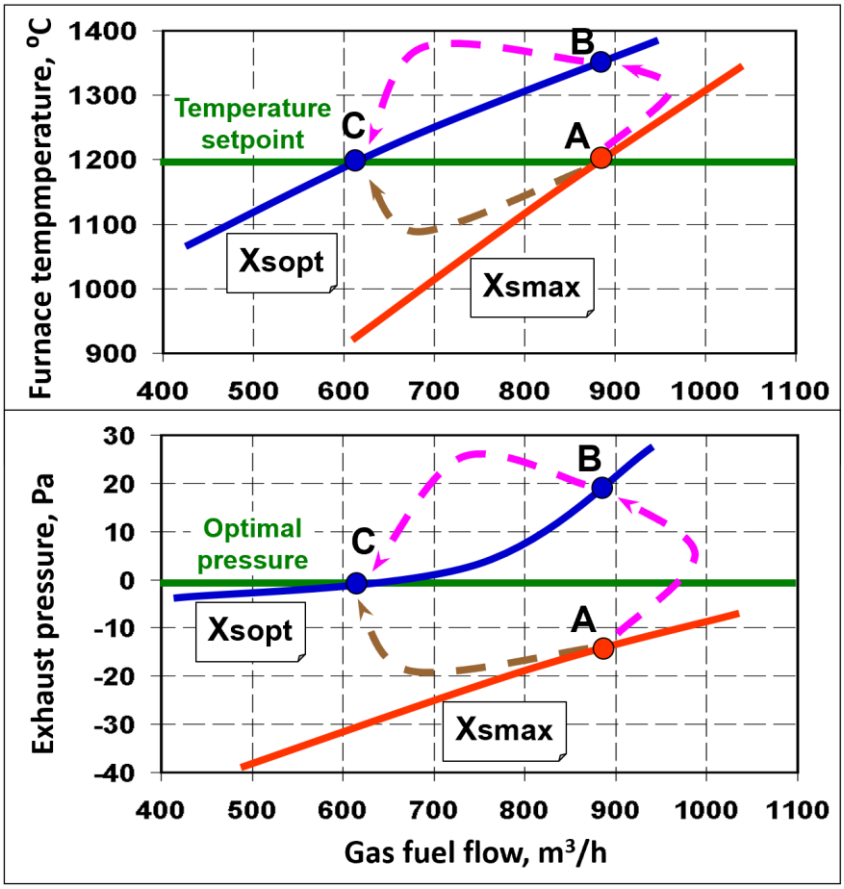

Fig. 2. Regulating temperature and pressure characteristics of the heating furnace

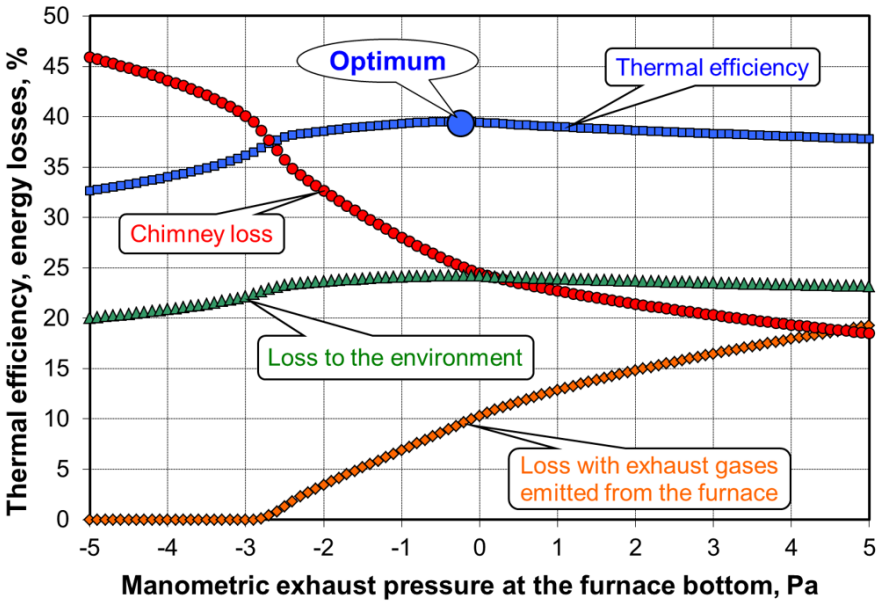

Fig. 3. Energy characteristics of the heating furnace

Publisher: **KOMAG Institute of Mining Technology, Poland**
© 2023 Author(s). This is an open access article licensed under the Creative Commons BY-NC 4.0 (https://creativecommons.org/licenses/by-nc/4.0/)

3.2. Operating tests of pressure control in the combustion chamber

The object of operational research was a step stove in which square bars 150 x 150 x 2300 mm are heated before plastic processing (rolling) to a temperature in accordance with the requirements of the technological process, and the feed is placed in contact in the furnace in two rows.

The furnace is fired with high-methane natural gas with the following parameters: heat of combustion W_g = 39 MJ/m^3, calorific value W_d = 35 MJ/m^3.

Furnace operating parameters:

- average temperature of warming-up zone furnace 1300ºC,
- average temperature of heating zone 1300ºC,
- feed temperature 1200ºC,
- average combustion air temperature 230ºC,
- heating zone burners – ceiling flat-flame burners,
- warming-up zone burners – ceiling flat-flame burners,
- average exhaust gas temperature ahead of the recuperator 846ºC,
- average exhaust gas temperature after the recuperator 568ºC,
- achieved output 15 Mg/h,
- dimensions of the furnace chamber 11150 x 7540 x 1500 mm,
- dimensions of the furnace input and output window: 7540 x 400 mm,
- chimney height 21 m,
- internal diameter of the furnace 0.8 m,
- loop recuperator with exchange surface 47 m^2.

In the presented object, the exhaust gas pressure in the furnace chamber was controlled manually by the operator by changing the position of the chimney valve. As a result of the modernization, the exhaust gas pressure control system was equipped with an automatic system based on a PLC controller with an input module and a state-of-the-art measuring system consisting of an intelligent APR-2000 GALW differential pressure transmitter with the following technical data:

- set range: -10÷10 Pa,
- acceptable static overload 35 kPa,
- main error ≤ ±1%,
- temperature error for 10ºC ≤ ±0.1%,
- operating temperature range -25÷85ºC (ambient temperature), measured medium -40÷120ºC in direct measurement (above 120ºC, measurements using the extended impulse tube),
- 12÷30 V DC power supply in a two-wire system,
- current output signal 4÷0 mA + HART in a two-wire system.

As a result of the automatic control of exhaust gas pressure in the furnace chamber, the gas consumption decreased from 55.5 m^3_N/Mg do 52.6 m^3_N/Mg, what means reduction in gas fuel consumption by 43.5 m^3_N/h. Assuming that price of natural gas is 1.83 PLN/m^3 [4] the savings are as follows:

- daily about 1 911 PLN,
- monthly about 57 300 PLN,
- yearly about 698 000 PLN.

Publisher: **KOMAG Institute of Mining Technology, Poland**
© 2023 Author(s). This is an open access article licensed under the Creative Commons BY-NC 4.0 (https://creativecommons.org/licenses/by-nc/4.0/)

Each CER unit represents 1 Mg of CO_2 and is a universal unit for measurement to indicate the global warming potential of greenhouse gases. Each not emitted tonne of CO_2 can be sold on the emission allowances market as a CER.

723 Mg of CO_2 was not emitted into the atmosphere per year, which can be used on the CO_2 emission allowances market getting additional funds for the company development or its modernization [3, 4, 5].

3.3. Summary of the problems related to pressure control in the combustion chamber

The main reason for failure to maintain the proper distribution of exhaust gas pressure in the combustion chamber of a metallurgical heating furnace is the lack of automatic pressure control and problems in determining its optimal value. It is not possible to manually control the exhaust gas pressure to a satisfactory level.

Maintaining the proper exhaust gas pressure in the heating furnace allows for achieving significant energy savings, which has been confirmed by the operational tests of the step stove. As a result of changing the manual control of exhaust gases pressure to automatic control, gas consumption was reduced and significant financial savings were achieved.

4. Conclusions

Energy and control analysis of the basic problem of excessive consumption of gaseous fuel in installations and systems used in the metallurgical energy industry, as well as operational tests on the basis of which a possibility of solving the problem were indicated. The analysis regarding the work subject was carried out for the sample industrial metallurgical heating furnace and concerned an economic aspect related to the environmental protection.

The basic and discussed problem was pressure control in the combustion chamber. The presented solution increases the energy efficiency of the heating furnace, which translates into significant economic effects while reducing CO_2 emissions, thus also constituting an important, pro-ecological solution.

Additionally, the results of the presented solution can be used in diagnostics and in designing the installations for the industrial furnaces, taking into account their long-term operation.

References

[1] https://www.europarl.europa.eu/news/pl [accessed: 07.10.2023]

[2] https://op.europa.eu/webpub/eca/special-reports/emissions-trading-system-18-2020/pl/ [accessed: 07.10.2023]

[3] https://www.kobize.pl/uploads/materialy/materialy_do_pobrania/raport_co2/2023/KOBiZE_Analiza_rynku_CO2_czerwiec_2023.pdf [accessed: 07.10.2023]

[4] https://tge.pl/ [accessed: 02.10.2023]

[5] https://pl.investing.com/commodities/carbon-emissions [accessed: 02.10.2023]

[6] Revun, M.P., Zinchenko, V.Y., Ivanov, V.I. et al.: „Optimal Thermal Control of a Chamber Furnace". Steel in Translation 48, 505–508 (2018). https://doi.org/10.3103/S0967091218080120

[7] Weiren, M., Kuangdi, X.: „Pusher-Type Heating Furnace, Structure and Classification of". The ECPH Encyclopedia of Mining and Metallurgy, 2022 Springer, Singapore. https://doi.org/10.1007/978-981-19-0740-1_84-1

[8] https://www.auma.com/pl/?no_redirect=1 [accessed: 05.10.2023]

[9] Niu, S.S., Xiao, D.: „Process Control Overview". Process Control. Advances in Industrial Control (2022). Springer, Cham. https://doi.org/10.1007/978-3-030-97067-3_1

[10] Tomeczek J.: Termodynamika, Wydawnictwa Politechniki Śląskiej, Gliwice, 1999

Publisher: **KOMAG Institute of Mining Technology, Poland**
© 2023 Author(s). This is an open access article licensed under the Creative Commons BY-NC 4.0 (https://creativecommons.org/licenses/by-nc/4.0/)

[11] Wnęk M.: Digital modification of chimney gate valve characteristics as a way to reduce the fuel consumption and CO2 emission. Metal 2019, s. 2020-2026. https://doi.org/10.37904/metal.2019.994

[12] Puszer A., Rozpondek M., Wnęk M.: Cyfrowa linearyzacja charakterystyki regulacyjnej przepustnicy kominowej. X Jubileuszowe Seminarium Naukowe „Nowe technologie i materiały w metalurgii i inżynierii materiałowej" Politechnika Śląska, Katowice 2002, s. 217

[13] Wnęk M.: Cyfrowa linearyzacja przepływowej charakterystyki regulacyjnej zasuwy kominowej. Hutnik, 1 (2016), s. 18-22

Publisher: **KOMAG Institute of Mining Technology, Poland**
© 2023 Author(s). This is an open access article licensed under the Creative Commons BY-NC 4.0 (https://creativecommons.org/licenses/by-nc/4.0/)